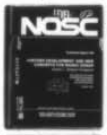
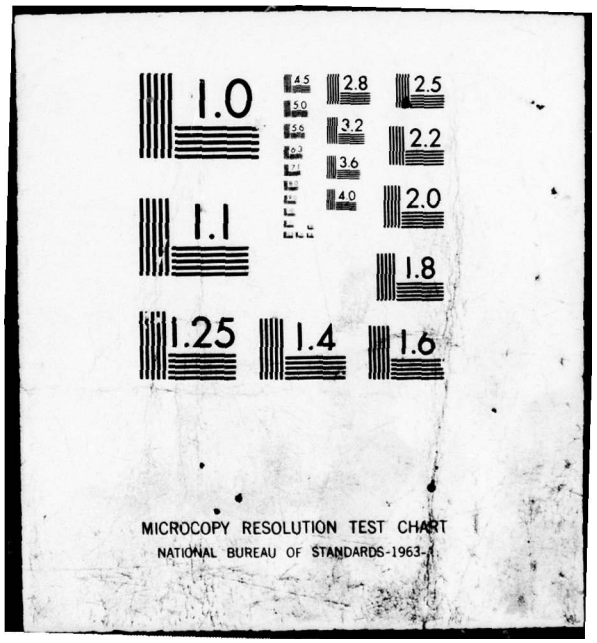
AD-A072 940 ORINCON CORP LA JOLLA CALIF F/G 17/1
FURTHER DEVELOPMENT AND NEW CONCEPTS FOR BIONIC SONAR. VOLUME 1--ETC(U)
OCT 78 R A ALTES, W J FAUST, R W FLOYD N66001-78-C-0080
UNCLASSIFIED OC-R-78-A004-1-VOL-1 NOSC-TR-404-VOL-1 NL

1 OF 1
AD A072940






END
DATE FILMED
9-79
DDC


1.0
1.1
1.25
1.4
1.6
1.8
2.0
2.2
2.5
2.8
3.2
3.6
4.0
4.5
5.0
5.6
6.3
MICROCOPY RESOLUTION TEST CHART
NATIONAL BUREAU OF STANDARDS-1963-A

LEVEL II

BS 12

# NOSC

NOSC TR 404
VOLUME 1

NOSC TR 404
VOLUME 1

AD A072940

**Technical Report 404**

# FURTHER DEVELOPMENT AND NEW CONCEPTS FOR BIONIC SONAR

## Volume 1 - Software Processors

RA Altes and WJ Faust
ORINCON Corporation
RW Floyd, NOSC
(Contract Monitor)

DDC
RECEIVED
AUG 21 1979
C

October 1978

DDC FILE COPY

Approved for public release; distribution unlimited

NAVAL OCEAN SYSTEMS CENTER
SAN DIEGO, CALIFORNIA 92152

NAVAL OCEAN SYSTEMS CENTER, SAN DIEGO, CA 92152

AN ACTIVITY OF THE NAVAL MATERIAL COMMAND

RR GAVAZZI, CAPT, USN
Commander

HL BLOOD
Technical Director

## ADMINISTRATIVE INFORMATION

The work reported here was performed by Richard A. Altes and W. J. Faust, ORINCON Corporation, 3366 No. Torrey Pines Ct., Suite 320, La Jolla, CA 92037 under Contract Number N-66001-78-C-0080. R. W. Floyd, Code 512, was the contract monitor.

The work was reported in three volumes. This document contains volume 1 of the report, reproduced in its entirety.

Released by

Dr. JF FISH, Head
Bioacoustics and Bionics Division

Under authority of

HO PORTER, Head
Biosciences Department

UNCLASSIFIED

SECURITY CLASSIFICATION OF THIS PAGE (When Data Entered)

# REPORT DOCUMENTATION PAGE

READ INSTRUCTIONS BEFORE COMPLETING FORM

1. REPORT NUMBER: NOSC TR-404 Volume 1
2. GOVT ACCESSION NO.: Final rept.
3. RECIPIENT'S CATALOG NUMBER:
4. TITLE (and Subtitle): FURTHER DEVELOPMENT AND NEW CONCEPTS FOR BIONIC SONAR, VOLUME 1, SOFTWARE PROCESSORS,
5. TYPE OF REPORT & PERIOD COVERED: FINAL FY 78,
6. PERFORMING ORG. REPORT NUMBER: OC-R-78-A004-1-VOL-1
7. AUTHOR(s): RA Altes and WJ Faust, ORINCON Corporation; RW Floyd, NOSC (Contract Monitor)
8. CONTRACT OR GRANT NUMBER(s): N66001-78-C-0080
9. PERFORMING ORGANIZATION NAME AND ADDRESS: ORINCON CORPORATION, 3366 No. Torry Pines Ct., Suite 320, La Jolla, CA 92037
10. PROGRAM ELEMENT, PROJECT, TASK AREA & WORK UNIT NUMBERS: PE6271/ SF11-121-491
11. CONTROLLING OFFICE NAME AND ADDRESS: Naval Ocean Systems Center, Hawaii Laboratory, PO Box 997, Kailua, Hawaii 96734
12. REPORT DATE: October 1978
13. NUMBER OF PAGES: 62
14. MONITORING AGENCY NAME & ADDRESS (if different from Controlling Office): NAVSEA 0342 (F. Romano), Arlington, VA 22314
15. SECURITY CLASS. (of this report): Unclassified
15a. DECLASSIFICATION/DOWNGRADING SCHEDULE:
16. DISTRIBUTION STATEMENT (of this Report): Richard A. Altes, W. J. Faust, R. W. Floyd

Approved for public release; distribution unlimited.

17. DISTRIBUTION STATEMENT (of the abstract entered in Block 20, if different from Report)
18. SUPPLEMENTARY NOTES
19. KEY WORDS (Continue on reverse side if necessary and identify by block number)

Bionics
Optimum detectors
Signal processing
Sonar
Spectrogram correlation
Target transfer function

20. ABSTRACT (Continue on reverse side if necessary and identify by block number)

This report documents theoretical studies of models of echolocation signal processing of dolphins and the testing of the effectiveness of these models for detecting and classifying small objects in introduced noise and reverberation. This volume describes the theoretical and software development of three models. The first, bionic components, is based on recognizing target features predicted by the geometric theory diffraction. The second method was a principal component analysis of a spectrogram, and the third was the principal →

(Continued)

DD FORM 1 JAN 73 1473 EDITION OF 1 NOV 65 IS OBSOLETE S/N 0102-LF-014-6601

UNCLASSIFIED

SECURITY CLASSIFICATION OF THIS PAGE (When Data Entered)

392 776

20. (Continued)

component analysis of a Fourier-Mellin transform. These algorithms have been tested by computing misclassification probabilities in noise and bottom reverberation. These tests indicate that the spectrogram model gives the best performance, with a probability of misclassification of $\leq$ of 0.1 occurring for SNR $\geq$ 0 dB and SCR (signal to clutter ratio) $\geq$ 6 dB.

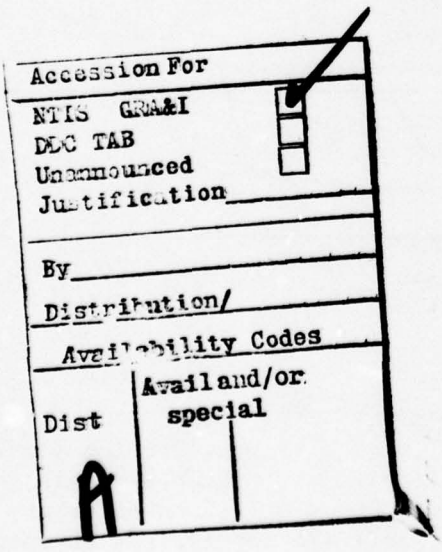


TABLE OF CONTENTS

Volume 1. SOFTWARE PROCESSORS


| | | Page |
|---|---|---|
| 1.1 | Introduction . . . . . | 1 |
| 1.2 | The "Bionic Component" Model. . . . . | 4 |
| 1.3 | The Spectrogram Model . . . . . | 12 |
| 1.4 | The Fourier-Mellin Transform Model . . . . . | 28 |
| 1.5 | Comparative Performance of Software Processors . | 35 |
| 1.6 | Conclusion . . . . . | 43 |
| 1.7 | References for Volume 1. . . . . | 44 |
| 1.8 | Appendices for Volume 1. . . . . | 48 |
| | A. Fortran Program for Construction of a Short-Duration Spectrogram . . . . . | 48 |
| | B. Fortran Program for Generating FM-Gram . . | 55 |


TABLES


| | | |
|---|---|---|
| 1. | Geometrical diffraction theory applied to scattering centers (monostatic case) . . . . . | 6 |
| 2. | List of targets that were used for the three software processors. . . . . | 18 |
| 3. | Sixteen largest normalized eigenvalues of $C_s$ and $C_{FM}$ in descending order . . . . . | 20 |
| 4. | Performance of the spectrogram correlator at 0 dB SNR or 0 dB SCR for 5, 7, and 9 principal components. . . . . | 42 |

TABLE OF CONTENTS (Continued)

Page

FIGURES


1. Idealized Wiener filters $\hat{W}_m(\omega)$ are defined as $\hat{W}_m(\omega) = \max[\omega^m |U(\omega)|^2 - c, 0]$ where c is the cross-over level for the amplitude normalized echo components with power spectral densities $\omega^m |U(\omega)|^2$, m = -2, ..., 2 . . . . . 8

2. Component detector output versus time for three different targets . . . . . 10

3. a. Sampled spectrogram of the match-filtered echo from a solid aluminum biconic (frustrum of a cone) . . . . . 15

   b. Sampled spectrogram of the match-filtered echo from a solid aluminum sphere, 3" diameter . . . . . 16

   c. Sampled spectrogram of the match-filtered echo from a hollow aluminum cylinder, 1.5" diameter x 7" long x 3/16" thick, broadside aspect . . . 17

4. Principal components or basis functions for the analysis of echo spectrograms. Figure 4a shows the component with the largest eigenvalue; Figure 4g shows the component with the seventh largest eigenvalue . . . . . 21

5. a. FM-gram samples for the echo from a solid aluminum biconic (frustrum of a cone). Largest response (98) occurs at output of filter No. 4 . . . . . 31

   b. FM-gram samples for the echo from a solid aluminum 3" sphere. Largest response (98) occurs at output of filter No. 7 . . . . . 33

   c. FM-gram samples for the echo from a hollow cylinder (1.5" x 7" x 3/16" wall thickness). Largest response (98) occurs at output of filter No. 3 . . . . . 34

TABLE OF CONTENTS (Continued)

Page

FIGURES (Continued)

6. Relative performance of software algorithms in additive white noise . . . . . 39

7. Relative performance of software algorithms in additive reflections from bottom clutter . . . . . 40

# I. SOFTWARE PROCESSORS

## 1.1 Introduction

This report discusses improved software bionic sonar implementations (Volume 1), spectrogram analysis (Volume 2), and the development of some new concepts that have been suggested by a study of animal sonar systems (Volume 3).

The software implementations in Volume 1 have followed two different philosophies for sonar target recognition. The first philosophy is based upon the idea that the various components in an echo can be theoretically predicted from the geometrical theory of diffraction, and that echoes can be classified by detecting these components and by determining their relative times of occurrence. This philosophy has led to the so-called "bionic component" method.

The second philosophy for software target classification is to empirically determine the important target components by analyzing the echoes from a variety of objects. The important components can be ascertained by means of principal component analysis.

The biological aspect of the "bionic component" method arises because the various theoretical components are best detected with a bank of proportional bandwidth filters when a dolphin-like pulse is used as a signal. There is evidence that some mammalian auditory processes can be modelled with such a filter bank.

The biological aspect of the principal component method arises from the domain in which echoes are analyzed and components are derived. The peripheral auditory system apparently forms a spectrogram-like representation of a sonar echo. Another domain

for echo representation is suggested by the relevance of a Fourier-Mellin transform to models of hearing. Principal component classifiers for both spectrogram and Fourier-Mellin echo representations have been implemented in software.

Three different software algorithms for bionic echo classification (bionic component detection, principal component spectrogram analysis, and principal component Fourier-Mellin transform analysis) have been tested against one another by computing misclassification probabilities in noise and bottom reverberation. These tests indicate that the spectrogram representation gives the best performance, with a probability of misclassification $\leq 0.1$ occurring for SNR $\geq$ 0 dB and SCR (signal-to-clutter ratio) $\geq$ 6 dB.

The superior experimental performance of a spectrogram correlator indicates that this method should be analyzed further from both optimum detector and biological modelling viewpoints. This analysis is the subject of Volume 2.

It is demonstrated in Volume 2 that spectrogram correlation is a locally optimum detection operation for low SNR signals that have been passed through a random, time-varying filter (e.g., a range-extended sonar target and/or a long-range or shallow-water propagation channel), in a Gaussian noise background. For non-Gaussian noise, the local optimality of the process is preserved by changing the power law that is associated with the envelope detection operation, i.e., by correlating stored data with a modified spectrogram.

Detection and estimation performance of the spectrogram correlation process is predicted and compared with behavioral data in Volume 2. Green's summation law for human detection of a sum of gated sinusoids is consistent with the expected performance

of a spectrogram correlator, and Siebert's description of the behavioral standard deviation of an auditory frequency estimate in humans is also consistent with a spectrogram correlator model. Neither of the above behavioral results is consistent with a matched filter model.

In the "new concepts" category, the following results have been obtained, and are discussed in detail in Volume 3:

1. A new, range-angle ambiguity function has been formulated in order to combine signal and array optimization for high resolution sonar. The new ambiguity function helps to demonstrate how increased system bandwidth can offset structural array constraints (two ears, separated by a small distance) in animal sonar systems.

2. A feasibility study has indicated that bats and dolphins may be able to estimate cross-range velocity when targets are less than 1 m. away. This capability may provide the animals with a counter-countermeasure to cope with evasive maneuvers. In a man-made system, the measurement of cross-range velocity at longer distances can be accomplished with more powerful sonars that have larger time-bandwidth products, coherent pulse-to-pulse integration, or an array that is larger than an animal's interaural distance.

3. A test is proposed to distinguish a locally optimum version of the energy spectrum analyzer of R. A. Johnson from a matched filter model for animal echolocation.

In the remainder of this volume, three different software processors or computerized models for animal sonar systems are discussed and compared. The discussions include a justification of each model in terms of biological results, as well as a description

of the signal processing operations that are performed. Target classification performance of the models is then compared for various levels of background noise and bottom reverberation.

## 1.2 The "Bionic Component" Model

The stimulus features that are important to an animal can be hypothesized by observing the differences in signals that would be useful for stimulus classification. In the case of echolocation, the stimulus is an echo and stimulus classification depends upon differences between echoes from various targets. By using modern pattern recognition techniques,[1] it is possible to empirically determine important classification features by obtaining a large data base of echoes from objects in the animal's environment. It is also possible to use theoretical predictions of target scattering characteristics in order to decide which echo features should be most important. The "bionic component" technique uses the latter philosophy.

Research on the prediction of target scattering characteristics has resulted in two main theoretical approaches. Geometrical and physical optics have evolved into a technique that is known as the geometrical theory of diffraction.[2-8] This theory involves the prediction of scattering characteristics from separate structures such as the tip of a cone or an edge, and it includes creeping wave effects (i.e., waves that propagate around the surface of the object). The echo components from various target structures are combined with proper delay, in order to form the composite echo. The geometrical theory of diffraction is primarily a high frequency approach for wavelengths that are smaller than the target.

The second approach to target scattering prediction is the use of natural modes or resonances, as derived, for example, with the singularity expansion technique.[9-13] Natural modes tend to dominate the trailing edge of an echo, whereas specular components (mirror-like reflections or glints) with higher amplitudes are found at the beginning of the echo. The advantage of natural mode characterization is that the resonant frequencies are independent of aspect, and it would thus seem that the target echo need not be modelled as an aspect-dependent random process. Experimental results with various sonar targets, however, have shown that, although natural resonances may be independent of aspect, the excitation of a given resonance and the energy that is re-radiated toward the receiver is, in fact, aspect-dependent. Furthermore, the trailing edge of the echo tends to be attenuated relative to the specular parts of the echo. Finally, the trailing edge of an echo is difficult to analyze if the target is immersed in clutter.

According to Bechtel and Ross,[8] the geometrical theory of diffraction predicts that many scattering centers will have cross-sections that vary as $\lambda^n$, where $\lambda$ is wavelength and $-2 \leq n \leq 2$. See Table 1. If cross section varies as $\lambda^n$, then the associated range-dependent transfer function must vary as a half-power of frequency, and the echo spectrum is $(j\omega)^{n/2}U(\omega)$ for $-2 \leq n \leq 2$, where $U(\omega)$ is the Fourier transform of the transmitted signal. An idealized highlight echo can be synthesized by passing an impulse through a filter with transfer function $(j\omega)^{n/2}U(\omega)$. The parameter n is range dependent, and changes from one highlight to the next. (A highlight is a local maximum in the echo envelope.) Since targets are distributed in azimuth and elevation as well as in range, it is possible that more than one type of geometry in Table 1 will

Table 1. Geometrical diffraction theory applied to scattering centers (monostatic case). *

| Type of Scattering Center | Radar Cross Section Dependence | | | Typical Targets |
|---|---|---|---|---|
| | Wavelength | Polarization | Aspect | |
| a) Edge diffraction | $\lambda$ | Major | Major | Rectangular flat plate, finite cylinder, truncated cone |
| b) Tip diffraction | $\lambda^2$ | Minor | Minor | Tip of a truncated cone, corners of flat plate |
| c) Surface diffraction | $e^{-\alpha\lambda^{-2/3}}$ | Major | Minor | Small cross section bodies, e.g., sphere-capped cone |
| d) Specular reflection (convex) | $\lambda^0$ | None | None (or minor) | Sphere (spheroid) |
| | $\lambda^{-1}$ | Minor | Major | Finite cylinder (broadside) |
| | $\lambda^{-2}$ | None | Major | Finite cylinder (axial), flat plate (broadside) |
| e) Reflex scattering (concave) | - | - | - | Corner reflector, intersection of cylinders |

*From Bechtel and Ross, Cornell Aeronautical Lab. Report ER/RIS-10.

be encountered in a given range interval. In this case, an idealized target is modelled by a sum of two or more different transfer functions.

Recent experimental results[14] seem to indicate that a highlight is rarely comprised of an echo from a single point in range. Sonar highlights are caused by range-distributed impedance changes. An echo from a range-distributed structure can be simulated by passing time-gated shot noise (closely spaced delta functions with uncorrelated epochs) through a filter that has a range-dependent transfer function. In terms of the geometrical theory of diffraction, highlight echoes are best modelled by passing time-gated shot noise, rather than a single impulse, through a filter with transfer function $(j\omega)^{n/2}U(\omega)$, where $-2 \leq n \leq 2$ and $U(\omega)$ is the spectrum of the transmitted signal. This random aspect of the model leads to a receiver that is different from the original "bionic sonar" proposed by Altes.[15]

A method of target characterization that is based upon the above model is to implement a detector that decides whether a given echo component is present at any given range. Since each echo component is modeled as a sample function of a random signal with known power spectral density, the detection can be implemented with an estimator-correlator process.[16]

The estimation part of the process consists of passing echo data through each of five Wiener filters. Since any given echo component constitutes an independent, interfering signal for the reception of a different component, the filters tend to be narrowband, and the $m^{th}$ filter transfer function is centered near the

maximum point of the power spectral density $|(j\omega)^{m/2}U(\omega)|^2$ of the $m^{th}$ echo component. Idealized versions of the five filters can be obtained by slicing the overlapping echo components at their cross-over levels in the frequency domain, as shown in Figure 1. The idealized estimating filters are

$$\hat{W}_m(\omega) = \max\left[|(j\omega)^{m/2}U(\omega)|^2 - c,\ 0\right],$$

$$m = -2,\ -1,\ 0,\ 1,\ 2 \qquad (1)$$

where c is the cross-over level that is shown in Figure 1.

The correlation part of the process is accomplished by multiplying each filter output by the original data and integrating over the expected duration of the highlight echo. The integrator

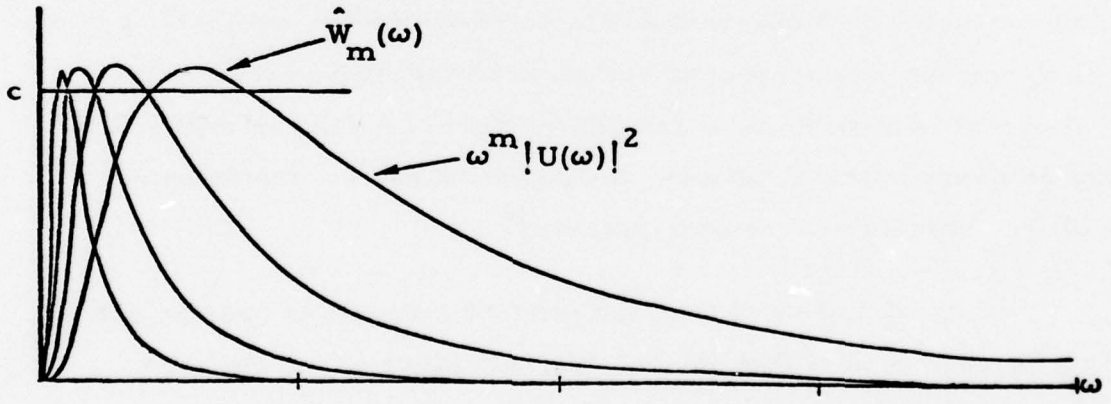



Figure 1. Idealized Wiener filters $\hat{W}_m(\omega)$ are defined as $\hat{W}_m(\omega) = \max[\omega^m|U(\omega)|^2 - c,\ 0]$ where c is the cross-over level for the amplitude normalized echo components with power spectral densities $\omega^m|U(\omega)|^2$, m = -2, ..., 2.

output must exceed two separate thresholds in order to trigger a decision that the $m^{th}$ component is present at any given range.

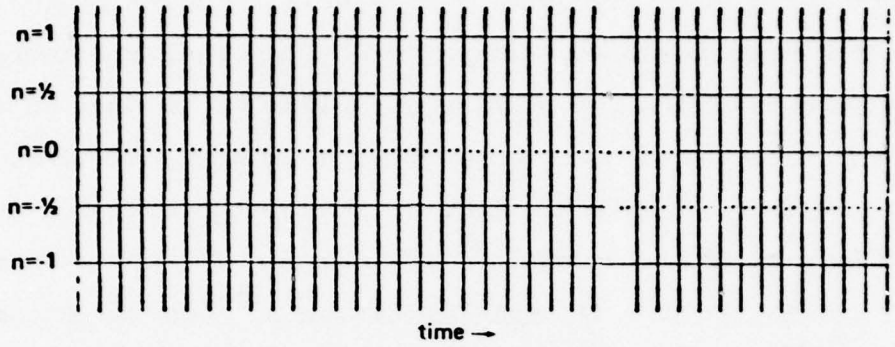
The first threshold is determined by expected echo energy. The second threshold varies with range, and is set to nine-tenths of the largest estimator-correlator response at any given time. The purpose of the second threshold is to compensate for the cross-talk or excitation of the $m^{th}$ filter by the $n^{th}$ echo component. From Figure 1, it is apparent that the $n^{th}$ component can excite the $m^{th}$ filter, even if the filter transfer functions do not overlap.

Application of the detection algorithm to a sonar echo results in a pattern of suprathreshold responses, as shown in Figure 2. Different patterns are obtained for different targets, and the patterns resemble a one-bit quantization of a spectrogram.

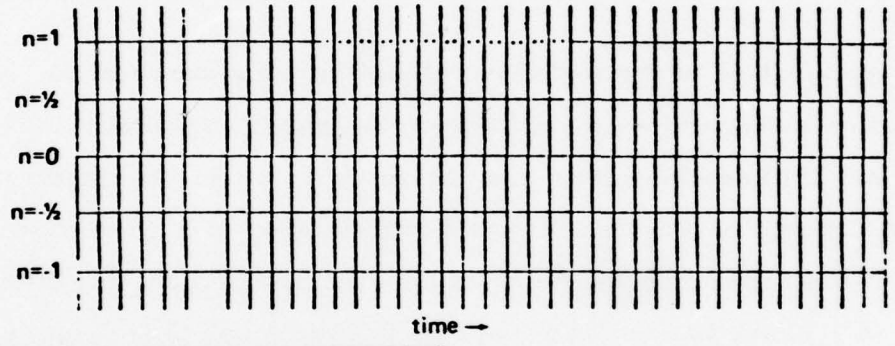
If the signal has log-normal spectral amplitude, the filters $\hat{W}_m(\omega)$ in (1) have bandwidths that are proportional to frequency. The existence of proportional bandwidth filters in mammalian auditory systems can be inferred from the results of noise-masking experiments[17] and from neurophysiological data.[18-20] Many cetacean echolocation signals have spectral magnitudes that are approximately log-normal in shape.[15]

In a previous report,[14] only the total number of suprathreshold responses from each filter was used for target classification. This method disregards the relative timing information that appears in Figure 2. It was therefore decided to add a timing parameter that describes the mean time for all the suprathreshold responses relative to the mean time for the filter that has the largest number of responses. This timing parameter, along with the number of detections from each filter, resulted in six target features altogether. The timing parameter is computed as follows.

A. ECHO FROM FRUSTRUM OF A CONE




B. 3" SPHERE ECHO




C. 1.5 x 7 x 3/16" AL CYLINDER ECHO

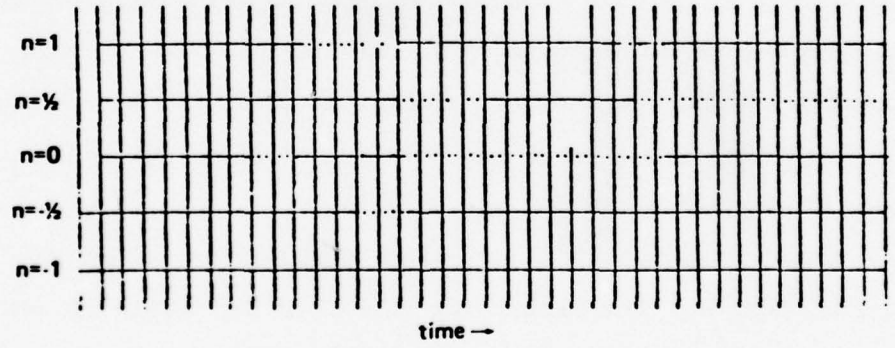



Figure 2. Component detector output versus time for three different targets.

Let $z_{ij}$ be the response of the $j^{th}$ detector at time $t_i$. If the response exceeds threshold, then $z_{ij} = 1$, and $z_{ij} = 0$ otherwise. The mean time for the suprathreshold responses from the $j^{th}$ filter is then

$$T_j = \sum_i t_i z_{ij} / \sum_i z_{ij} \ .$$

Suppose that the maximum number of detections is observed at the output of detector number J. The mean time of all the suprathreshold detector responses relative to $T_J$ is then

$$\Delta T = \sum_{j=1}^{5} T_j - T_J = \sum_{\substack{j=1 \\ j \neq J}}^{5} T_j \ . \qquad (2)$$

The timing parameter $\Delta T$ in (2) is an extra feature that was used to generate new misclassification probabilities for the bionic component method. The performance of this algorithm will be compared with that of the other two models in Section 1.5. The five-component system without $\Delta T$ will also be included in the comparison.

## 1.3 The Spectrogram Model

A spectrogram is a display of a sequence of short duration energy density spectra, and it portrays the distribution of signal energy in both frequency and time. A spectrogram-like signal representation may be formed by the peripheral auditory system.[21-23] The use of the spectrogram in sonar echo processing depends upon the integration time, i.e., the duration of the time window or the impulse response duration of the filters that are used to generate a sequence of energy density spectra. When the spectrogram is formed by a bank of filters with envelope detected responses, the integration time varies inversely with the bandwidth of each filter. Unfortunately, there is a large spread of possible bandwidths and integration times that have been measured by noise-masking experiments, frequency discrimination studies, and neurophysiological investigations. It would appear, in fact, that bandwidth (and integration time) depends upon the particular detection problem that is presented to a subject.[24,25]

If long integration times are relevant, then both a transmitted pulse and the resulting echoes are included in the Fourier transform, and the Johnson-Titlebaum model[26] seems to be appropriate. For very short integration times, one can divide up a target into a sequence of range cells, and observe the evolution of reflected spectral energy as a function of range. Both long and short integration times have certain advantages, but we consider only a short integration time in this volume.

The window length for our software algorithm is 9 cm long in range, and a new window is generated every 1.8 cm. One aspect of the software spectrogram processor may not be particularly "bionic." Before echoes are time-windowed and Fourier transformed,

they are passed through a filter that is matched to the transmitted signal. Since the time-bandwidth product of the signal (a typical dolphin pulse) is not very large, this operation is probably optional. For test purposes, however, it was decided that matched filtering would improve the temporal resolution of the spectrogram.

A Fortran program for computing a spectrogram for wideband sonar echo analysis is listed in Appendix A.

It has been mentioned that an alternative to theoretical scattering prediction is to use empirical echo data in order to obtain a set of features for target classification. The weakness of such an approach is that the data base that is used for feature definition may be too limited. On the other hand, the use of wideband signals upon targets that are made of different materials can severely degrade the reliability of theoretical predictors. Short-term spectrogram analysis has therefore been coupled with empirical feature determination.

Features are significant attributes of the data that can be used for classification. Consider a filter that processes the data in order to extract a particular feature. A set of such filters with orthogonal impulse responses would constitute an orthogonal basis for decomposition of the data. Since the desired number of features is limited in practice, the orthogonal basis set is generally incomplete, i.e., it is not capable of reconstructing every possible data waveform. One can obtain a "best" incomplete N-dimensional basis set by finding the set that gives the least expected mean-square error between the reconstructed data and a representative set of the original data, for a given number of feature vectors (orthogonal filters), N. The resulting set of N feature vectors are the N eigenvectors of the data covariance matrix that have the largest eigenvalues.[27]

The associated eigenvalues are indicative of the amount of information that is contributed by each feature vector, i.e., the percentage of the total data variance that is accounted for by each component.

Application of the "best" incomplete basis set corresponds to a Karhounen-Loève decomposition of the data, and it is also known as a principal component analysis.[1] Since a limited number of basis functions are used to convey the maximum possible information about the data, one can assume (in the absence of a better approach) that these basis functions correspond to the most important features for classification

Typical spectrogram responses to various echoes are shown in Figure 3. A sampled two-dimensional plot can be represented as a long column vector by sequentially listing the elements in the first row, then the second row, etc. A column vector of this kind was constructed from the echo spectrogram of each of the 37 targets in Table 2. The resulting set of column vectors was then used to construct a data covariance matrix, $C_s$. If $\underline{d}_i$ is the column vector that is derived from the spectrogram of the $i^{th}$ echo, then

$$C_s = \frac{1}{37} \sum_{i=1}^{37} (\underline{d}_i - \bar{\underline{d}})(\underline{d}_i - \bar{\underline{d}})^T \qquad (3)$$

where the T denotes transpose and

$$\bar{\underline{d}} = \frac{1}{37} \sum_{i=1}^{37} \underline{d}_i . \qquad (4)$$

The target-induced variation in the magnitude of the spectrogram at each point, i.e., the variation that is caused by different echoes, thus contributes to the derivation of a feature set.

KMAX= 58

| | | | | | | | | | | | | | | | | | | | | | | | | | | | |
|---|---|---|---|---|---|---|---|---|---|---|---|---|---|---|---|---|---|---|---|---|---|---|---|---|---|---|---|
| 0 | 0 | 0 | 0 | 0 | 0 | 0 | 0 | 0 | 0 | 0 | 0 | 0 | 0 | 0 | 0 | 0 | 0 | 0 | 0 | 0 | 0 | 0 | 0 | 0 | 0 | 0 | 0 |
| 0 | 0 | 0 | 0 | 0 | 0 | 0 | 0 | 0 | 0 | 0 | 0 | 0 | 0 | 0 | 0 | 0 | 0 | 0 | 0 | 0 | 0 | 0 | 0 | 0 | 0 | 0 | 0 |
| 0 | 0 | 0 | 0 | 0 | 0 | 0 | 0 | 0 | 0 | 0 | 0 | 0 | 0 | 0 | 0 | 0 | 0 | 0 | 0 | 0 | 0 | 0 | 0 | 0 | 0 | 0 | 0 |
| 0 | 0 | 0 | 0 | 0 | 0 | 0 | 0 | 0 | 0 | 0 | 0 | 0 | 0 | 0 | 0 | 0 | 0 | 0 | 0 | 0 | 0 | 0 | 0 | 0 | 0 | 0 | 0 |
| 0 | 0 | 0 | 0 | 0 | 0 | 0 | 0 | 0 | 0 | 0 | 0 | 0 | 0 | 0 | 0 | 0 | 0 | 0 | 0 | 0 | 0 | 0 | 0 | 0 | 0 | 0 | 0 |
| 0 | 0 | 0 | 1 | 0 | 0 | 0 | 0 | 0 | 0 | 0 | 1 | 0 | 0 | 0 | 0 | 0 | 0 | 0 | 0 | 0 | 0 | 0 | 0 | 0 | 0 | 0 | 0 |
| 0 | 1 | 0 | 8 | 1 | 1 | 0 | 0 | 0 | 2 | 4 | 3 | 0 | 0 | 0 | 0 | 0 | 0 | 0 | 0 | 0 | 0 | 0 | 0 | 0 | 0 | 0 | 0 |
| 4 | 4 | 1 | 29 | 13 | 5 | 0 | 2 | 7 | 17 | 22 | 11 | 0 | 1 | 1 | 2 | 2 | 0 | 1 | 3 | 4 | 1 | 0 | 0 | 0 | 1 | 0 | |
| 10 | 7 | 3 | 64 | 39 | 18 | 5 | 10 | 28 | 52 | 60 | 33 | 9 | 8 | 10 | 13 | 10 | 5 | 8 | 14 | 15 | 8 | 3 | 3 | 4 | 4 | 1 | |
| 13 | 9 | 4 | 83 | 60 | 34 | 21 | 28 | 56 | 91 | 98 | 63 | 31 | 24 | 27 | 29 | 26 | 20 | 24 | 31 | 28 | 18 | 11 | 10 | 10 | 7 | 3 | |
| 9 | 7 | 4 | 65 | 52 | 38 | 32 | 40 | 65 | 94 | 98 | 73 | 46 | 34 | 35 | 37 | 36 | 33 | 36 | 38 | 33 | 23 | 16 | 14 | 13 | 9 | 4 | |
| 4 | 3 | 2 | 29 | 25 | 23 | 24 | 30 | 44 | 57 | 60 | 50 | 35 | 27 | 25 | 27 | 29 | 30 | 30 | 27 | 22 | 16 | 12 | 10 | 9 | 7 | 4 | |
| 0 | 0 | 0 | 6 | 5 | 6 | 8 | 12 | 15 | 19 | 20 | 19 | 14 | 11 | 9 | 11 | 12 | 14 | 13 | 11 | 8 | 5 | 4 | 4 | 4 | 3 | 2 | |
| 0 | 0 | 0 | 0 | 0 | 0 | 1 | 1 | 2 | 2 | 2 | 3 | 2 | 1 | 1 | 2 | 2 | 3 | 2 | 2 | 1 | 0 | 0 | 0 | 0 | 0 | 0 | |
| 0 | 0 | 0 | 0 | 0 | 0 | 0 | 0 | 0 | 0 | 0 | 0 | 0 | 0 | 0 | 0 | 0 | 0 | 0 | 0 | 0 | 0 | 0 | 0 | 0 | 0 | 0 | |
| 0 | 0 | 0 | 0 | 0 | 0 | 0 | 0 | 0 | 0 | 0 | 0 | 0 | 0 | 0 | 0 | 0 | 0 | 0 | 0 | 0 | 0 | 0 | 0 | 0 | 0 | 0 | |

frequency →

time →

AT LINE 297
>EXIT
EDIT 297 LINES OUTPUT

**Figure 3a. Sampled spectrogram of the match-filtered echo from a solid aluminum biconic (frustrum of a cone).**

```
KMAX=   94
     0   0   0   0   0   0   0   0   0   0   0   0   0   0   0   0   0   0   0   0   0   0   0   0   0   0
     0   0   0   0   0   0   0   0   0   0   0   0   0   0   0   0   0   0   0   0   0   0   0   0   0   0
     0   0   0   0   0   0   0   0   0   0   0   0   0   0   0   0   0   0   0   0   0   0   0   0   0   0
     0   0   0   0   0   0   0   0   0   0   0   0   0   0   0   0   0   0   0   0   0   0   0   0   0   0
     0   0   0   1   1   0   0   0   0   0   0   0   0   0   0   0   0   0   0   0   0   0   0   0   0   0
     0   0   0   2   4   0   0   1   2   4   2   0   0   0   0   0   0   0   0   0   0   0   0   0   0   0
     0   0   0   5  14   8   7  15  16  13   5   1   0   0   0   0   0   0   0   0   0   0   0   0   0   0
     0   0   0  10  34  38  39  51  45  24   8   4   4   3   1   0   0   0   0   0   0   0   0   0   0   0
     0   0   1  18  57  79  86  93  74  30   5   7  11   8   1   0   0   0   0   0   0   0   0   0   0   0
     0   0   4  25  66  93  98  98  79  29   0   9  18  14   4   0   1   1   0   0   0   0   0   0   0   0
     0   1   6  24  51  65  61  61  54  25   3  10  20  16   7   3   2   2   1   0   0   0   0   0   0   0
     0   1   5  15  25  25  19  19  23  17   8   9  14  12   7   4   3   2   1   0   0   0   0   0   0   0
     0   0   2   5   6   4   1   2   5   7   6   5   6   5   4   2   1   1   0   0   0   0   0   0   0   0
     0   0   0   0   0   0   0   0   0   1   2   1   1   1   1   1   0   0   0   0   0   0   0   0   0   0
     0   0   0   0   0   0   0   0   0   0   0   0   0   0   0   0   0   0   0   0   0   0   0   0   0   0
     0   0   0   0   0   0   0   0   0   0   0   0   0   0   0   0   0   0   0   0   0   0   0   0   0   0
EOF AT LINE 297
297*>EXIT
END EDIT 297 LINES OUTPUT
```

frequency →

time →

**Figure 3b. Sampled spectrogram of the match-filtered echo from a solid aluminum sphere, 3" diameter.**

```
KMAX=   72
    0   0   0   0   0   0   0   0   0   0   0   0   0   0   0   0   0   0   0   0   0   0   0   0   0
    0   0   0   0   0   0   0   0   0   0   0   0   0   0   0   0   0   0   0   0   0   0   0   0   0
    0   0   0   0   0   0   0   0   0   0   0   0   0   0   0   0   0   0   0   0   0   0   0   0   0
    0   0   0   0   0   0   0   1   0   0   0   0   0   0   0   0   0   0   0   0   0   0   0   0   0
    0   0   0   0   1   0   3   2   0   0   0   0   0   0   0   0   0   0   0   0   0   0   0   0   0
    0   0   0   2   6   7  13   6   0   0   0   0   0   0   0   0   0   0   0   0   0   0   0   0   0
    0   0   0   4  18  28  30  14   2   3   1   0   0   0   0   0   0   0   0   0   0   0   0   0   0
    0   0   0   8  39  63  43  18  13  15  12   8   5   4   4   4   2   1   1   1   0   1   1   0
    0   0   0  13  63  93  40   8  25  38  37  28  21  17  14  11   7   4   3   2   2   2   2   1
    0   0   1  18  73  98  35   0  32  59  61  50  39  30  23  16   9   6   4   3   3   3   3   2
    0   0   2  18  60  75  35   9  31  55  58  50  40  30  21  13   7   4   3   2   2   2   2   2
    0   0   2  13  33  41  29  18  22  30  31  28  23  17  11   6   3   1   1   1   1   0   1   1
    0   0   2   6  11  14  14  12   9   9   8   7   6   4   2   1   0   0   0   0   0   0   0   0
    0   0   0   1   2   2   3   3   1   1   0   0   0   0   0   0   0   0   0   0   0   0   0   0
    0   0   0   0   0   0   0   0   0   0   0   0   0   0   0   0   0   0   0   0   0   0   0   0
    0   0   0   0   0   0   0   0   0   0   0   0   0   0   0   0   0   0   0   0   0   0   0   0
EOF AT LINE 297
297*>EXIT
END EDIT 297 LINES OUTPUT
```

frequency →

time →

**Figure 3c. Sampled spectrogram of the match-filtered echo from a hollow aluminum cylinder, 1.5" diameter x 7" long x 3/16" thick, broadside aspect.**

Table 2. List of targets that were used for the three software processors.

Unless otherwise noted, targets are broadside to the direction of propagation. Broadside - 0°, end-on = 90°. Cylinder dimensions are diameter x length x wall thickness. Hollow cylinders are open-ended (water-filled).

5" biconic

3" sphere

2.5 x 7" rock cyl.

1.5 x 7 x 3/16" Al. cyl.

1.5 x 7 x 4/16" Al. cyl.

1.5 x 7 x 5/16" Al. cyl.

1.5 x 7 x 6/16" Al. cyl.

3 x 7 x 2/16" Al. cyl.

3 x 7 x 4/16" Al. cyl.

3 x 7 x 6/16" Al. cyl.

3 x 7 x 8/16" Al. cyl.

3 x 7 x 10/16" Al. cyl.

3 x 7 x 8/16" PVC cyl.

Transmitted signal (planar target)

6 cm foam cube, 0°

6 cm foam cube, 45°

6 cm x 6 cm foam cyl., 0°

6 cm x 6 cm foam cyl., 90°

2.5 x 7" Al. cyl., 0°

2.5 x 7" Al. cyl., 5°

2.5 x 7" Al. cyl., 10°

2.5 x 7" Al. cyl., 15°

2.5 x 7" Al. cyl., 20°

2.5 x 7" Al. cyl., 25°

2.5 x 7" Al. cyl., 30°

2.5 x 7" Al. cyl., 35°

2.5 x 7" Al. cyl., 40°

2.5 x 7" Al. cyl., 45°

2.5 x 7" Al. cyl., 50°

2.5 x 7" Al. cyl., 55°

2.5 x 7" Al. cyl., 60°

2.5 x 7" Al. cyl., 65°

2.5 x 7" Al. cyl., 70°

2.5 x 7" Al. cyl., 75°

2.5 x 7" Al. cyl., 80°

2.5 x 7" Al. cyl., 85°

2.5 x 7" Al. cyl., 90°

Table 3 (middle column) shows the eigenvalue estimates for the first sixteen eigenvectors of $C_s$.

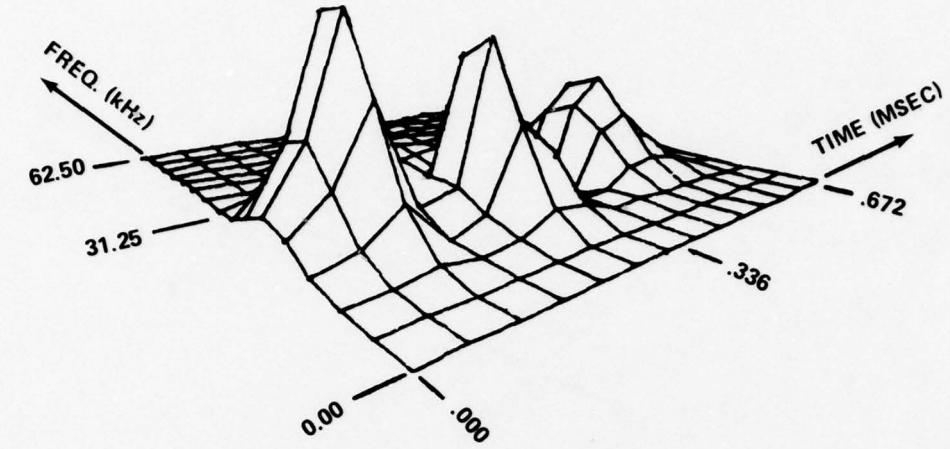
The first seven eigenvectors of $C_s$ are shown in Figure 4. These functions of frequency and time represent the features that are most useful for the classification of the targets in Table 2 from a spectrogram representation of wideband sonar echoes.

The functions in Figure 4 have interesting implications for models of the acoustic and visual systems. Suppose that each of the features in Figure 4 corresponds to a neuron in the auditory cortex. The neuron that is associated with Figure 4b, for example, has an inhibitory center at 40 kHz, surrounded by an excitatory area in frequency and time. The neuron in Figure 4c is excited by spectrogram outputs that appear early in time, and it is inhibited by outputs that appear later in time. Such neurons display not only lateral inhibition for neural "sharpening" in the frequency domain,[28] but also forward and/or backward masking in the time domain.[29] The similarity to receptive fields in vision[30] is obvious. Our results suggest that visual cells with specialized receptive fields may form an orthonormal basis for pattern recognition, and the well-known excitatory center/inhibitory surround cell is <u>one</u> of the principal components for such a basis.

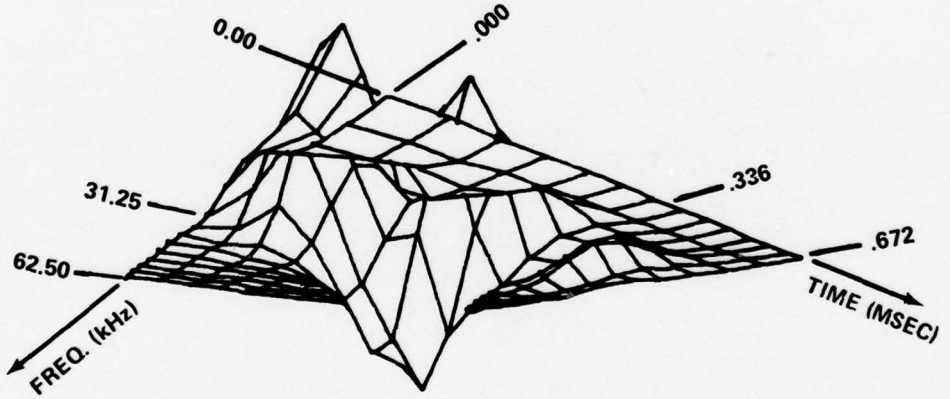
Before principal component analysis occurs, a data spectrogram must be registered in time, i.e., the temporal position of the data relative to the basis set must be determined. The basis set covers a frequency-time window that has dimensions 56 kHz x 672 $\mu$sec. If the match-filtered echo data is denoted $r(t_i)$, where the

Table 3. Sixteen largest normalized eigenvalues of $C_s$ and $C_{FM}$ in descending order.

| Eigenvalue Number | $C_s$ | $C_{FM}$ |
|---|---|---|
| 1 | .459 | .284 |
| 2 | .202 | .198 |
| 3 | .100 | .131 |
| 4 | .068 | .095 |
| 5 | .042 | .057 |
| 6 | .036 | .044 |
| 7 | .031 | .031 |
| 8 | .021 | .025 |
| 9 | .011 | .022 |
| 10 | .009 | .018 |
| 11 | .007 | .015 |
| 12 | .005 | .014 |
| 13 | .004 | .012 |
| 14 | .003 | .010 |
| 15 | .002 | .008 |
| 16 | .001 | .007 |



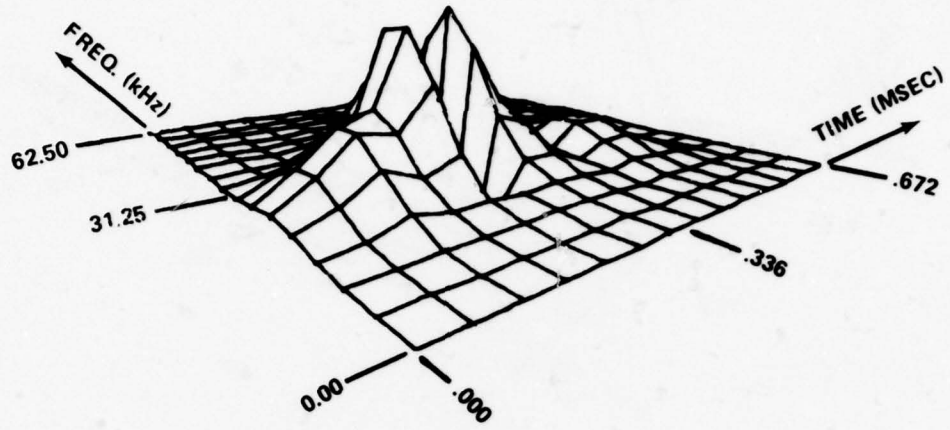

TOP VIEW



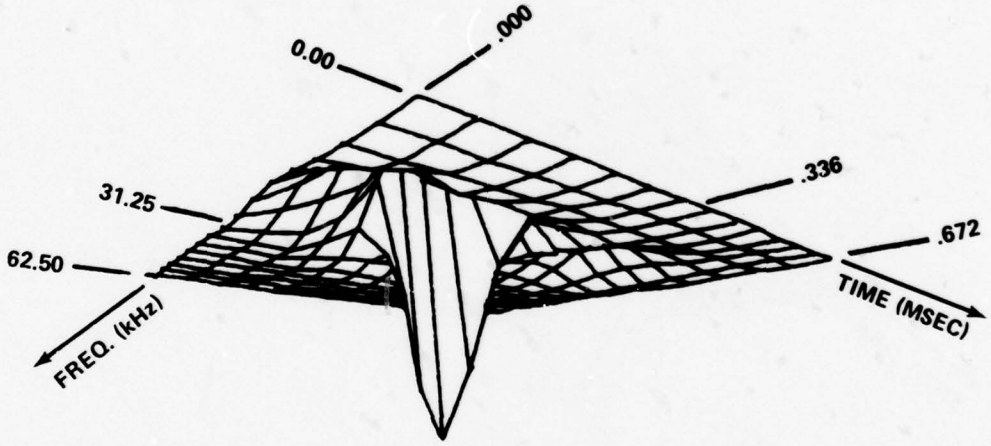

BOTTOM VIEW

Figure 4a.

Figure 4. Principal components or basis functions for the analysis of echo spectrograms. Figure 4a shows the component with the largest eigenvalue; Figure 4g shows the component with the seventh largest eigenvalue.

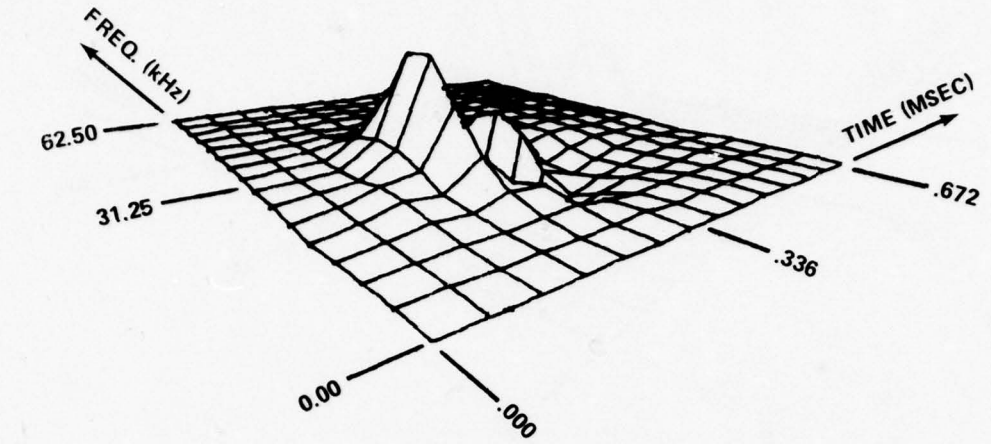



TOP VIEW

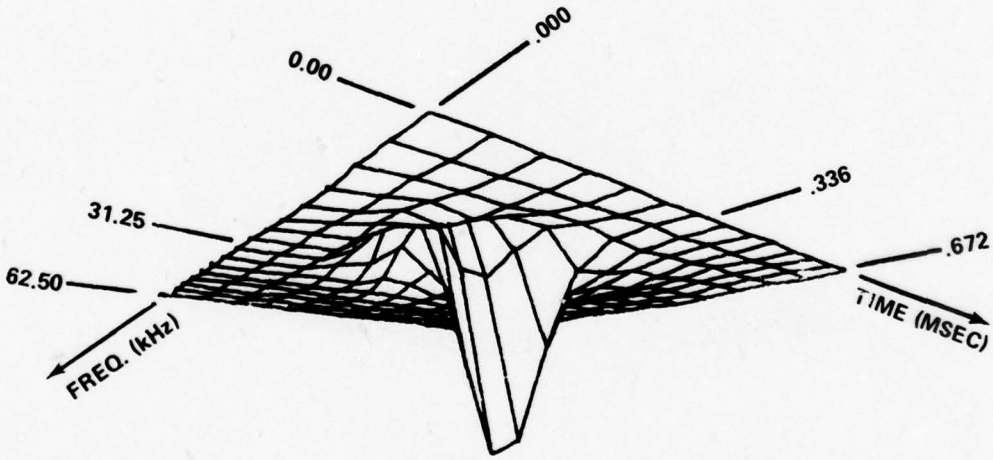



BOTTOM VIEW

Figure 4b.

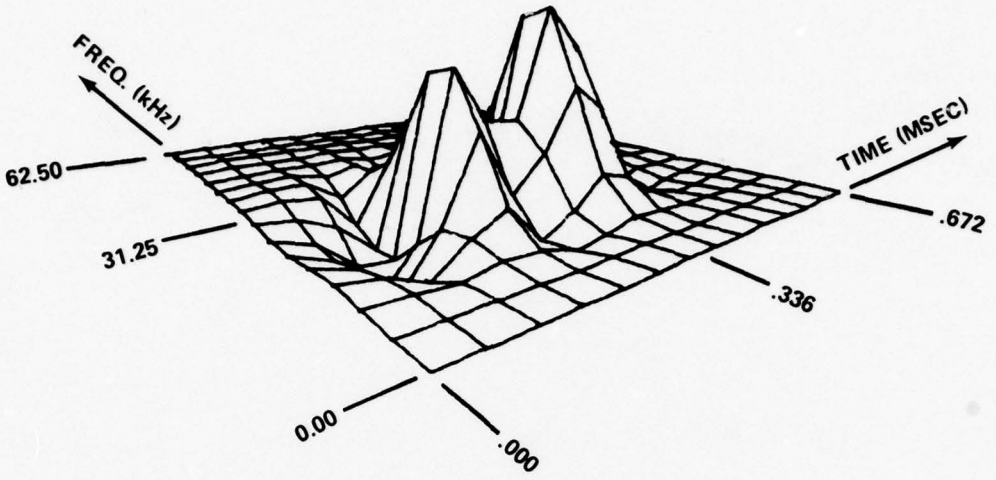



TOP VIEW

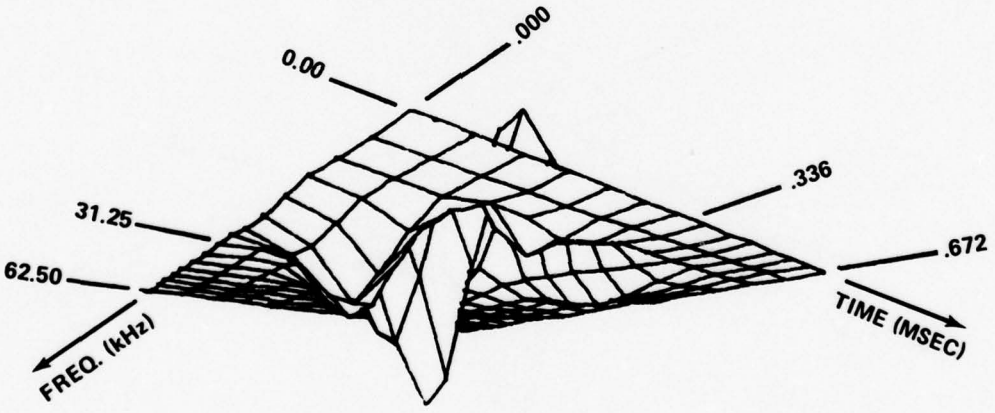



BOTTOM VIEW

Figure 4c.

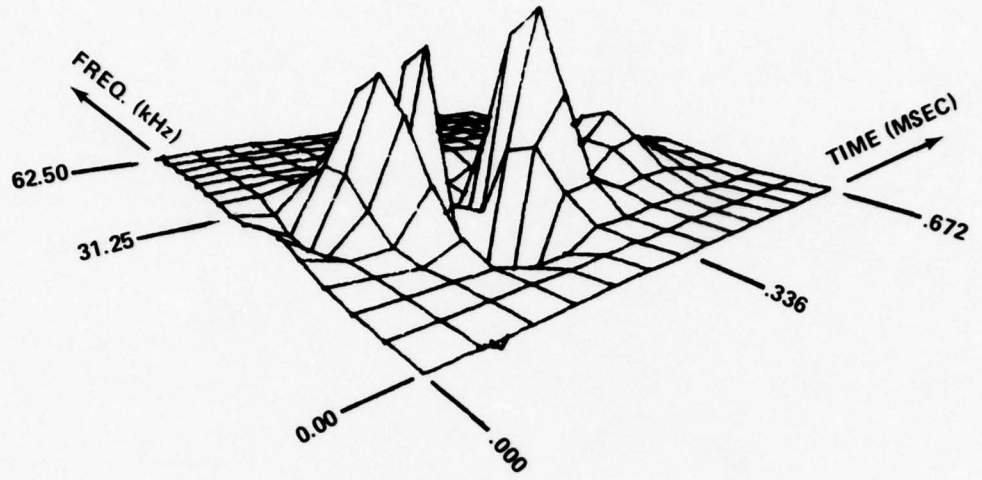



TOP VIEW

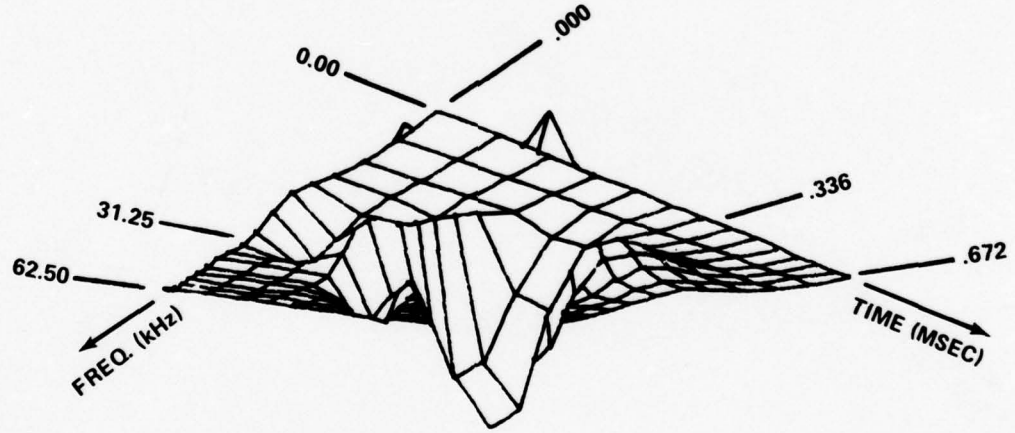



BOTTOM VIEW

Figure 4d.

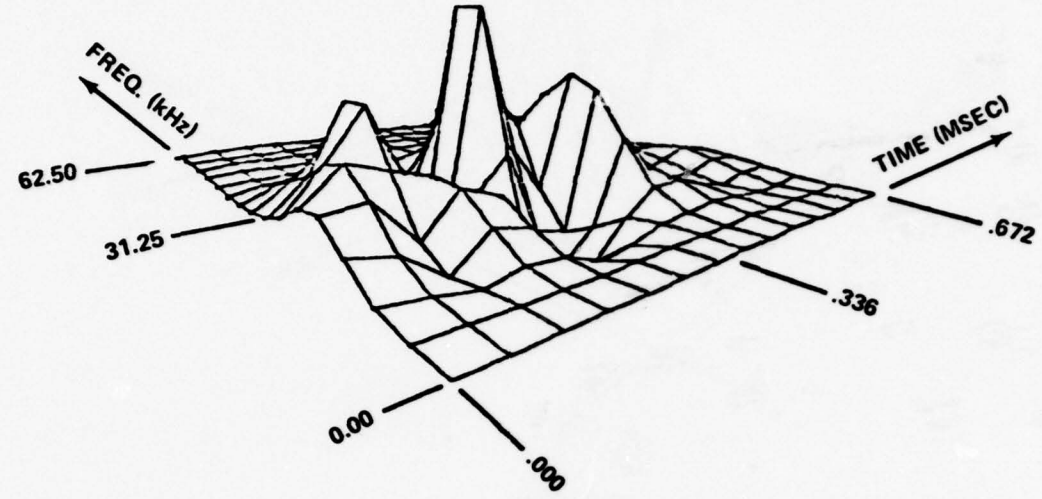



TOP VIEW

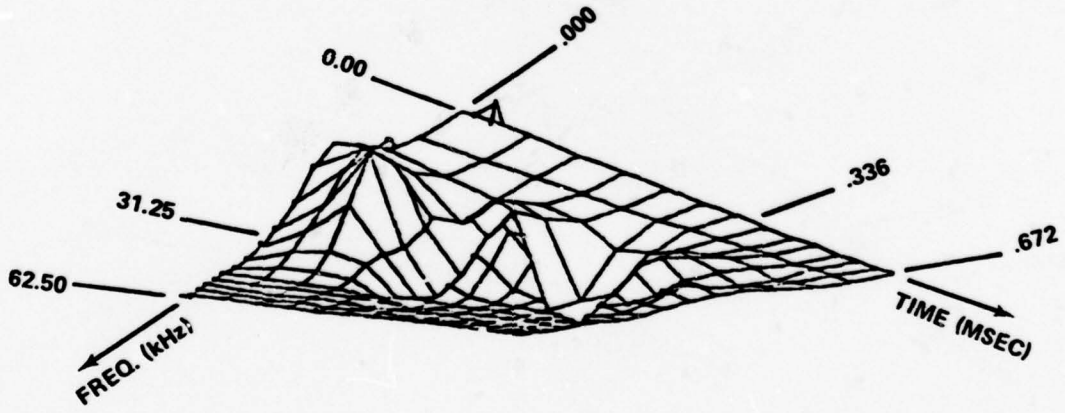



BOTTOM VIEW

Figure 4e.

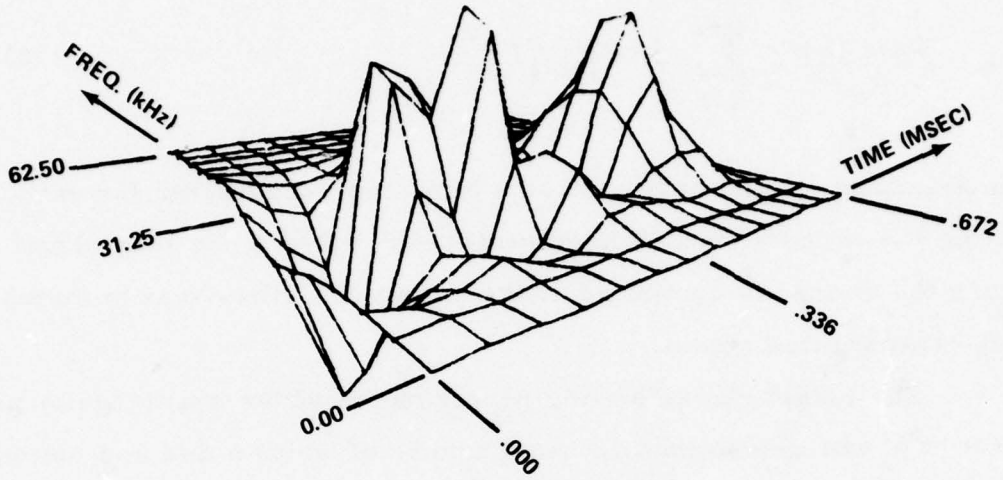



TOP VIEW

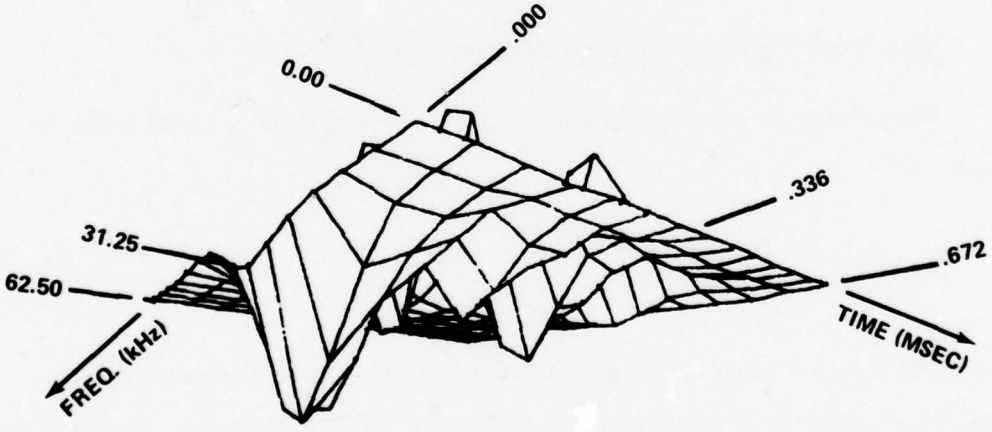



BOTTOM VIEW

Figure 4f.




TOP VIEW




BOTTOM VIEW

Figure 4g.

sampling interval is 24 μsec long, then the starting time for spectrogram analysis (i.e., the left-hand edge of the frequency-time window) corresponds to the point $t_j$ where

$$\text{sum}\,(t_j) = \sum_{i=1}^{28} \left[ r(t_{j+i-1}) \right]^2 \tag{5}$$

is maximized. The above sum is a local energy detector for estimating the range of an extended target with a 672 μsec long echo, where the energy is computed at the output of a filter that is matched to the transmitted signal.

The target classification performance of the spectrogram processor has been determined in backgrounds of white noise and bottom reverberation. This performance is compared to the other two software processors in Section 1.5.

## 1.4 The Fourier-Mellin Transform Model

The Fourier-Mellin transform of an analytic signal u(t) is defined as[31]

$$G_u(jx) = \int_0^\infty U(f)\, e^{jx \log(2\pi f)}\, df/f \tag{6}$$

where U(f) is the Fourier transform of u(t). This transform is relevant to biological systems because the phase function exp[jx log (2πf)] can be synthesized with a bank of proportional bandwidth filters,[31,32] and because the transform can be used to obtain a scale- and shift-invariant waveform representation.[31] The process in (6) is equivalent to matched filtering of a linear period modulated rectangular pulse,[31,33] i.e., a waveform that is used by some bats and dolphins for echolocation.[33-35]

A time-dependent, two-dimensional signal representation can be obtained from (6) by defining a set of band limited filters

$$V_k(f) = \begin{cases} f^{-1} \exp[j x_k \log(2\pi f)] \ , & f_L \leq f \leq f_H \\ 0 \ , \quad f < f_L \quad \text{or} \quad f > f_H \end{cases} \tag{7}$$

where $k = 1, 2, \ldots, M$.

The two-dimensional representation is then

$$F_{uv}(t_i, x_k) = \left| \int_{f_L}^{f_H} U(f)\, V_k(f)\, e^{j2\pi f t_i}\, df \right|^2 \tag{8}$$

A delayed signal $u(t-\tau)$ with Fourier transform

$$U(f) = \begin{cases} f^{-1} \exp[-j(2\pi f \tau + c \log(2\pi f)] \ , & f_L \leq f \leq f_H \\ 0 \ , \quad f < f_L \quad \text{or} \quad f > f_H \end{cases} \tag{9}$$

will be match-filtered by the process in (8), and the envelope-detected matched filter response will be observed on the $x_k = c$ profile of the function $F_{uv}(t_i, x_k)$. The maximum matched filter response will occur at $t_i = \tau$, $x_k = c$.

Another bionic aspect of the transformation in (8) is that the filters $V_k(f)$ are matched to rectangular pulses with different chirp rates, $x_k$. The existence in humans of filters that are chirp-rate-sensitive has been deduced by Kay and Mathews.[36]

The function

$$F_{uv}(t, x_k) = \left| \int_B U(f)\, V_k(f)\, e^{j2\pi ft}\, df \right|^2, \quad k = 1, 2, \ldots, M \qquad (10)$$

where

$$V_k(f) = \begin{cases} f^{-1} \exp[\, j x_k \log(2\pi f)\,] \;, & f \in B \\ 0, \text{ otherwise} \end{cases} \qquad (11)$$

will be called the FM-gram, since it is a modified spectrogram that is based upon the Fourier-Mellin transform rather than upon an ordinary spectral representation.

A Fortran program for computing the FM-gram is listed in Appendix B. Seven k-values were used, corresponding to

$$x_k = (k-3)\,(-0.25)\,(2\pi) \,/\, (\log 1.2), \quad k=1, 2, \ldots, 7. \qquad (12)$$

Examples of FM-gram echo representations for three targets are shown in Figure 5. Large differences between the three echo representations are immediately noticeable. If such large differences are found for each target, then one would expect that the various target representations are nearly orthogonal, and that a large number of principal components are needed in order to approximate all the echoes in the data set. This situation will be indicated by a relatively slow drop-off of the eigenvalues of the target covariance matrix, $C_{FM}$. This phenomenon can indeed be

Filter Number →

| n=1 | n=2 | n=3 | n=4 | n=5 | n=6 | n=7 |
|---|---|---|---|---|---|---|
| 0 | 0 | 1 | 0 | 0 | 0 | 0 |
| 0 | 0 | 0 | 0 | 0 | 0 | 0 |
| 1 | 0 | 0 | 0 | 0 | 0 | 0 |
| 1 | 1 | 0 | 0 | 0 | 0 | 0 |
| 0 | 1 | 0 | 0 | 0 | 0 | 1 |
| 0 | 0 | 0 | 0 | 0 | 0 | 1 |
| 0 | 0 | 0 | 0 | 0 | 1 | 1 |
| 0 | 0 | 0 | 0 | 0 | 2 | 1 |
| 0 | 0 | 0 | 0 | 0 | 2 | 5 |
| 0 | 0 | 0 | 1 | 1 | 4 | 7 |
| 0 | 0 | 1 | 3 | 3 | 4 | 4 |
| 0 | 0 | 1 | 4 | 5 | 5 | 2 |
| 0 | 1 | 1 | 4 | 9 | 8 | 4 |
| 0 | 2 | 2 | 3 | 9 | 8 | 5 |
| 3 | 3 | 4 | 3 | 7 | 6 | 5 |
| 10 | 2 | 5 | 4 | 4 | 4 | 7 |
| 9 | 4 | 5 | 6 | 4 | 2 | 6 |
| 2 | 8 | 4 | 7 | 4 | 1 | 3 |
| 0 | 5 | 3 | 5 | 4 | 1 | 2 |
| 0 | 0 | 4 | 3 | 3 | 2 | 1 |
| 4 | 0 | 3 | 3 | 2 | 4 | 1 |
| 16 | 7 | 1 | 3 | 1 | 3 | 2 |
| 37 | 23 | 2 | 3 | 1 | 2 | 2 |
| 50 | 43 | 20 | 4 | 2 | 1 | 1 |
| 46 | 58 | 48 | 5 | 4 | 2 | 1 |
| 47 | 65 | 60 | 14 | 7 | 3 | 0 |
| 59 | 54 | 56 | 40 | 11 | 5 | 1 |
| 61 | 34 | 45 | 61 | 18 | 7 | 3 |
| 46 | 25 | 32 | 54 | 32 | 9 | 8 |
| 27 | 24 | 20 | 38 | 54 | 16 | 17 |
| 13 | 19 | 11 | 27 | 58 | 28 | 26 |
| 6 | 11 | 8 | 19 | 38 | 49 | 32 |
| 3 | 5 | 11 | 11 | 20 | 74 | 37 |
| 2 | 3 | 12 | 6 | 13 | 74 | 43 |
| 1 | 2 | 8 | 5 | 13 | 38 | 47 |
| 1 | 1 | 3 | 6 | 10 | 10 | 47 |
| 1 | 1 | 2 | 7 | 8 | 4 | 38 |
| 1 | 1 | 1 | 4 | 7 | 5 | 18 |
| 0 | 1 | 1 | 2 | 7 | 4 | 5 |
| 0 | 2 | 1 | 2 | 4 | 4 | 5 |
| 1 | 2 | 2 | 4 | 1 | 5 | 13 |
| 3 | 3 | 3 | 6 | 1 | 6 | 13 |
| 8 | 4 | 6 | 9 | 4 | 6 | 10 |
| 16 | 9 | 11 | 12 | 10 | 8 | 12 |
| 31 | 19 | 17 | 14 | 15 | 18 | 15 |
| 49 | 32 | 28 | 18 | 22 | 42 | 17 |
| 59 | 46 | 45 | 25 | 36 | 58 | 27 |

↓ Time

Figure 5a. FM-gram samples for the echo from a solid aluminum biconic (frustrum of a cone). Largest response (98) occurs at output of Filter No. 4 (see next page).

Filter Number →

| n=1 | n=2 | n=3 | n=4 | n=5 | n=6 | n=7 |
|---|---|---|---|---|---|---|
| 59 | 68 | 64 | 37 | 51 | 51 | 47 |
| 51 | 86 | 71 | 56 | 66 | 48 | 64 |
| 42 | 82 | 68 | 80 | 82 | 53 | 57 |
| 36 | 61 | 65 | 98 | 88 | 51 | 36 |
| 30 | 38 | 58 | 94 | 81 | 45 | 27 |
| 24 | 23 | 40 | 68 | 62 | 42 | 26 |
| 21 | 16 | 23 | 42 | 38 | 37 | 24 |
| 19 | 12 | 15 | 22 | 18 | 27 | 21 |
| 16 | 10 | 12 | 8 | 7 | 17 | 23 |
| 12 | 10 | 12 | 3 | 3 | 9 | 26 |
| 9 | 10 | 11 | 2 | 1 | 4 | 21 |
| 7 | 10 | 9 | 3 | 1 | 1 | 13 |
| 7 | 8 | 7 | 3 | 1 | 1 | 7 |
| 9 | 8 | 5 | 3 | 3 | 2 | 4 |
| 10 | 9 | 3 | 3 | 6 | 5 | 5 |
| 11 | 10 | 2 | 3 | 7 | 10 | 9 |
| 10 | 9 | 2 | 4 | 7 | 20 | 12 |
| 8 | 6 | 3 | 6 | 8 | 24 | 14 |
| 6 | 4 | 5 | 8 | 10 | 19 | 15 |
| 5 | 2 | 7 | 12 | 12 | 15 | 14 |
| 4 | 2 | 8 | 15 | 16 | 14 | 11 |
| 2 | 2 | 7 | 14 | 18 | 12 | 7 |
| 1 | 2 | 7 | 11 | 18 | 9 | 7 |
| 1 | 3 | 7 | 8 | 15 | 7 | 8 |
| 1 | 4 | 8 | 6 | 8 | 5 | 6 |
| 1 | 6 | 9 | 7 | 5 | 3 | 4 |
| 3 | 8 | 10 | 9 | 4 | 2 | 2 |
| 6 | 12 | 10 | 10 | 4 | 2 | 1 |
| 13 | 18 | 12 | 11 | 4 | 3 | 1 |
| 21 | 22 | 15 | 10 | 4 | 4 | 1 |
| 26 | 23 | 15 | 9 | 3 | 5 | 1 |
| 25 | 21 | 15 | 8 | 4 | 5 | 2 |
| 21 | 15 | 12 | 7 | 5 | 3 | 3 |
| 16 | 9 | 8 | 4 | 5 | 3 | 4 |
| 12 | 5 | 5 | 3 | 6 | 2 | 4 |
| 7 | 3 | 2 | 2 | 5 | 3 | 5 |
| 4 | 2 | 1 | 1 | 3 | 3 | 5 |
| 2 | 1 | 0 | 1 | 1 | 3 | 5 |
| 2 | 1 | 0 | 1 | 0 | 3 | 5 |
| 1 | 0 | 0 | 1 | 0 | 2 | 3 |
| 1 | 0 | 0 | 1 | 0 | 1 | 1 |

Time ↓

Figure 5a. (Continued)

Filter Number →

| n=1 | n=2 | n=3 | n=4 | n=5 | n=6 | n=7 |
|---|---|---|---|---|---|---|
| 1 | 0 | 0 | 0 | 0 | 0 | 1 |
| 1 | 0 | 0 | 0 | 0 | 0 | 1 |
| 1 | 0 | 0 | 0 | 0 | 0 | 1 |
| 1 | 3 | 0 | 0 | 0 | 1 | 1 |
| 2 | 9 | 2 | 0 | 1 | 2 | 1 |
| 4 | 15 | 16 | 1 | 1 | 3 | 1 |
| 11 | 19 | 32 | 6 | 3 | 4 | 1 |
| 28 | 23 | 34 | 29 | 7 | 5 | 1 |
| 54 | 25 | 29 | 67 | 14 | 5 | 1 |
| 67 | 30 | 28 | 65 | 26 | 5 | 1 |
| 66 | 43 | 30 | 35 | 43 | 5 | 1 |
| 63 | 53 | 31 | 16 | 45 | 6 | 2 |
| 63 | 50 | 30 | 12 | 27 | 12 | 5 |
| 58 | 40 | 30 | 12 | 11 | 27 | 12 |
| 45 | 33 | 27 | 13 | 6 | 55 | 28 |
| 29 | 30 | 22 | 16 | 9 | 69 | 54 |
| 16 | 27 | 20 | 23 | 26 | 46 | 82 |
| 7 | 23 | 23 | 38 | 54 | 25 | 98 |
| 3 | 17 | 32 | 53 | 74 | 29 | 85 |
| 1 | 11 | 41 | 56 | 77 | 52 | 47 |
| 0 | 5 | 34 | 47 | 62 | 65 | 24 |
| 0 | 2 | 16 | 35 | 36 | 51 | 27 |
| 0 | 1 | 3 | 17 | 14 | 29 | 38 |
| 0 | 0 | 0 | 3 | 4 | 12 | 26 |
| 0 | 0 | 0 | 0 | 0 | 3 | 7 |
| 0 | 0 | 0 | 0 | 0 | 0 | 0 |
| 0 | 0 | 0 | 0 | 0 | 0 | 0 |
| 0 | 0 | 0 | 1 | 0 | 0 | 0 |
| 1 | 1 | 1 | 1 | 3 | 1 | 1 |
| 3 | 3 | 3 | 1 | 5 | 5 | 5 |
| 5 | 5 | 4 | 2 | 4 | 12 | 10 |
| 6 | 6 | 4 | 2 | 3 | 12 | 13 |
| 5 | 6 | 3 | 3 | 4 | 6 | 13 |
| 3 | 4 | 2 | 4 | 4 | 2 | 8 |
| 2 | 2 | 1 | 3 | 2 | 1 | 2 |
| 1 | 1 | 0 | 2 | 1 | 1 | 0 |
| 1 | 0 | 0 | 1 | 0 | 0 | 0 |

Time ↓

Figure 5b. FM-gram samples for the echo from a solid aluminum 3" sphere. Largest response (98) occurs at output of Filter No. 7.

Filter Number →

| n=1 | n=2 | n=3 | n=4 | n=5 | n=6 | n=7 |
|---|---|---|---|---|---|---|
| 4 | 0 | 0 | 0 | 0 | 0 | 1 |
| 11 | 0 | 0 | 0 | 0 | 1 | 1 |
| 24 | 1 | 1 | 0 | 0 | 2 | 2 |
| 35 | 13 | 10 | 0 | 2 | 3 | 3 |
| 35 | 49 | 16 | 6 | 5 | 5 | 4 |
| 23 | 80 | 22 | 33 | 12 | 8 | 5 |
| 11 | 64 | 52 | 74 | 24 | 12 | 7 |
| 6 | 29 | 98 | 67 | 45 | 16 | 9 |
| 4 | 8 | 79 | 40 | 66 | 21 | 11 |
| 2 | 1 | 21 | 33 | 53 | 25 | 13 |
| 0 | 0 | 1 | 24 | 19 | 24 | 14 |
| 0 | 0 | 0 | 4 | 3 | 18 | 13 |
| 0 | 0 | 0 | 0 | 0 | 8 | 9 |
| 0 | 0 | 0 | 0 | 0 | 1 | 4 |
| 2 | 1 | 1 | 3 | 0 | 0 | 1 |
| 4 | 5 | 1 | 3 | 3 | 0 | 0 |
| 7 | 8 | 4 | 2 | 11 | 0 | 0 |
| 9 | 10 | 8 | 2 | 13 | 3 | 2 |
| 11 | 10 | 9 | 3 | 6 | 16 | 5 |
| 13 | 9 | 7 | 6 | 3 | 33 | 8 |
| 13 | 7 | 5 | 9 | 4 | 22 | 14 |
| 10 | 6 | 4 | 8 | 7 | 5 | 29 |
| 6 | 5 | 4 | 6 | 9 | 2 | 36 |
| 4 | 4 | 4 | 4 | 9 | 5 | 16 |
| 3 | 2 | 4 | 4 | 6 | 9 | 1 |
| 2 | 2 | 4 | 4 | 3 | 8 | 0 |
| 2 | 2 | 3 | 3 | 2 | 5 | 4 |
| 1 | 2 | 2 | 2 | 2 | 2 | 8 |
| 1 | 2 | 2 | 2 | 2 | 1 | 5 |
| 1 | 2 | 2 | 1 | 2 | 1 | 2 |
| 1 | 2 | 1 | 1 | 1 | 1 | 1 |
| 1 | 1 | 1 | 0 | 1 | 1 | 0 |
| 2 | 1 | 1 | 1 | 0 | 1 | 0 |
| 1 | 1 | 0 | 1 | 0 | 0 | 0 |
| 1 | 0 | 0 | 0 | 0 | 0 | 0 |

↓ Time

Figure 5c. FM-gram samples for the echo from a hollow aluminum cylinder (1.5" x 7" x 3/16" wall thickness). Largest response (98) occurs at output of Filter No. 3.

observed in Table 3. The biological counterparts of the eigenvectors of $C_{FM}$ would be neural receptive fields that are inhibited or excited by frequency modulated pulses with various chirp rates and relative times of occurrence.

The target classification performance of the FM-gram processor has been determined in backgrounds of white noise and bottom reverberation. This performance is compared to the other software processors in the next section.

## 1.5 Comparative Performance of Software Processors

The performance of the three bionic target classifiers was determined by grouping targets into various classes and by computing probability of misclassification in a background of clutter (bottom reverberation) or white noise. Probability of misclassification for various signal-to-noise ratios (SNR) and signal-to-clutter ratios (SCR) were determined by adding clutter or noise to the target echoes and then processing the resulting data with each of the three software algorithms. SNR and SCR are defined as follows.

$$\text{SNR} = \text{echo energy} / \text{average noise power} \tag{13}$$

where the noise power is measured at the output of a bandpass filter with low frequency cutoff $f_L$ = 5 kHz and high frequency cutoff $f_H$ = 95 kHz. This filter simulates the pass band of the experimental sonar system that was used to gather the data. Similarly,

$$\text{SCR} = \text{echo energy} / \text{average clutter power} \tag{14}$$

where the clutter is a sample function of bottom reverberation. The reverberation was measured with a sonar signal that had a higher chirp rate than the signal u(t) that was used in obtaining target echoes. The reverberation data was therefore pre-processed in software in order to obtain clutter that would have been measured with u(t) as the transmitted signal. A large, anomalous low frequency clutter component was observed at 2 kHz, and this component was filtered out by passing clutter echoes through a bandpass filter with $f_L$ = 5 kHz and $f_H$ = 95 kHz. The clutter power is measured at the output of this bandpass filter.

The eigenvalues of $C_s$ in Table 3 decrease sufficiently rapidly that adequate performance can be obtained with only seven eigenfunctions. A classification test with seven eigenfunctions of $C_{FM}$ gives comparatively poor results. The reason for this relatively poor performance is that target information is more distributed for the FM-gram representation, and more basis vectors are needed in order to adequately describe each target. This effect is represented by the relatively even distribution of eigenvalue amplitudes for $C_{FM}$ in Table 3. The classification performance of an FM-gram representation has therefore been evaluated by using sixteen eigenfunctions rather than the seven that are used for the spectrogram representation.

Is it advantageous to "spread out" the target information among a comparatively large number of orthogonal components, or should one always use the representation that has the least number of basis vectors? The latter strategy corresponds to dimensionality reduction in a pattern recognition problem. The strategy of "spreading out" information corresponds to a high-diversity system as employed, for example, in spread-spectrum communication. By

using the Kullback-Leibler information number, R. F. Daly[37] has shown that an optimum degree of diversity is such as to make the signal-to-noise ratio for each orthogonal component equal to approximately 2. Daly's result suggests that better performance will be obtained at low SNR if the available echo energy can be concentrated among a few principal components, as in the spectrogram representation. As SNR is increased, a more diverse echo representation is permissible. We might therefore predict that the seven-component spectrogram analysis will be superior to FM-gram with sixteen principal components for low SNR. It will be seen that this prediction is commensurate with our experimental results.

Target echoes were classified by means of a mean-square distance measure

$$D_i = \sum_{n=1}^{N} (r_n - f_{ni})^2 \qquad (15)$$

where

$r_n$ = correlation between the spectrogram or FM-gram and the $n^{th}$ eigenvector, or the response of one of the five suprathreshold detection counters or the timing parameter for the "bionic component" method.

$f_{ni}$ = $n^{th}$ eigenvector correlator or "bionic component" response for the $i^{th}$ target in the absence of noise or reverberation (archetypes)

$N$ = 5 for the bionic component method without the timing parameter

= 6 for the bionic component method with the timing parameter

N = 7 for principal component spectrogram analysis

= 16 for principal component FM-gram analysis

If $D_i < D_n$, for all $n \neq i$, then the echo is classified as target i. A misclassification occurs when the test (15) judges a target to be a member of class B when the target has been assigned to class A, or vice-versa. If target i is wrongly identified as target j, no misclassification results if j is in the same class as i.

Probabilities of misclassification as a function of input SNR or SCR are shown in Figures 6 and 7. Figures 6a and 7a are concerned with distinguishing a 2.5 x 7" solid aluminum cylinder, as seen from various aspects, from a variety of other targets, which are listed in Table 2. Figures 6b and 7b display misclassification probabilities for a cylinder versus non-cylinder classifier, i.e., the targets in Table 2 are categorized as "cylinders" or "something else." Figures 6c and 7c show results for a metal versus non-metal classifier, again using the targets in Table 2.

The graphs in Figures 6 and 7 include probabilities that would be obtained by random guessing. These probabilities are computed from the equation

$$\Pr(\text{misclass'n}) = \Pr(\text{misclass'n}|A)\,\Pr(A) + \Pr(\text{misclass'n}|B)\,\Pr(B)$$

where the target set is divided into two classes A and B. Pr(A) is the probability that a target from class A is encountered and Pr(misclass'n|A) is the probability of misclassification given that a target from class A is the correct choice, and a random guess is made. For example, if A is the class of 32 cylinders and B is the

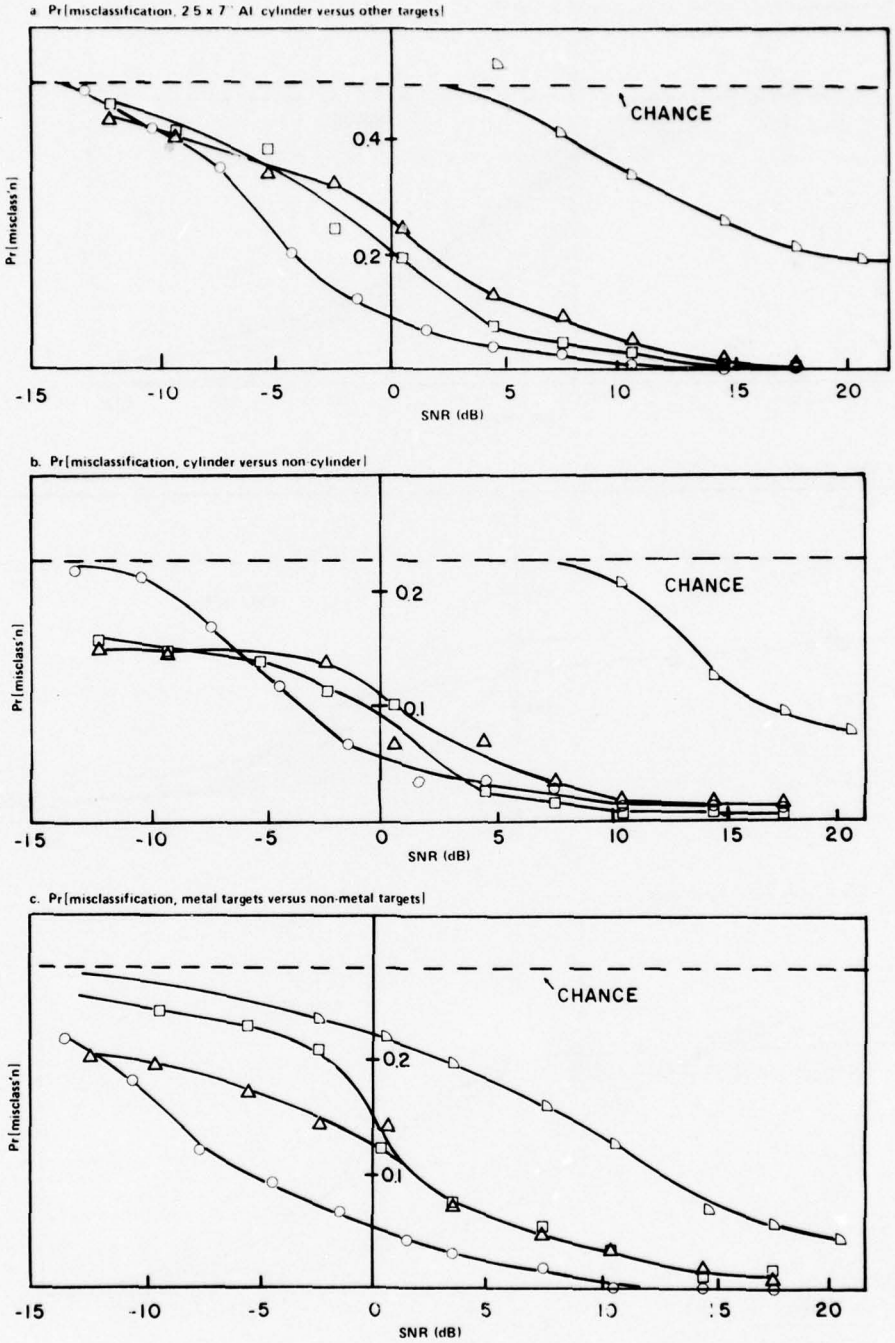



**Figure 6. Relative performance of software algorithms in additive white noise.**

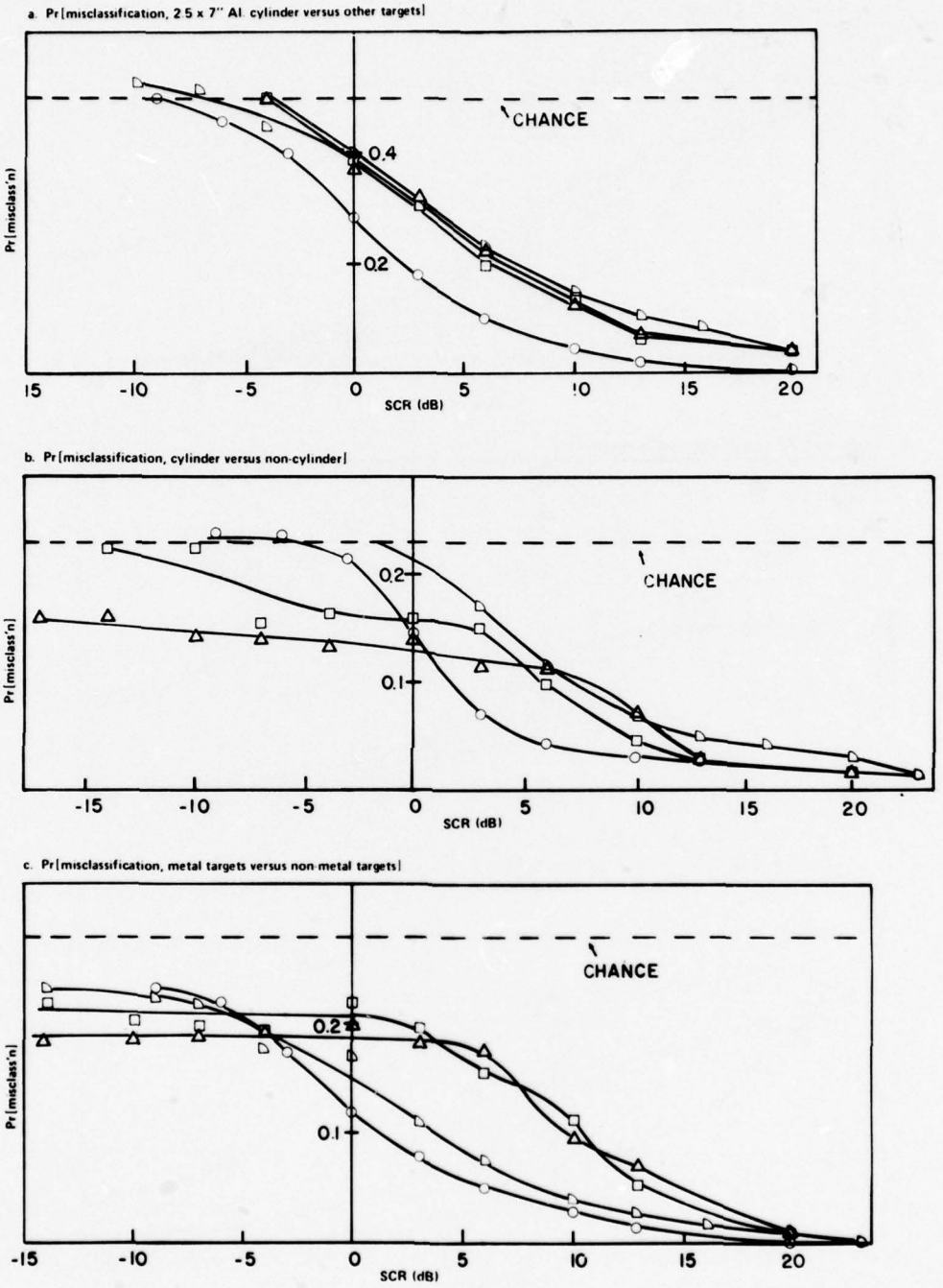



Figure 7. Relative performance of software algorithms in additive reflections from bottom clutter.

class of 5 non-cylinders in Table 2, then

$$\Pr(\text{misclass'n}) = \left(\frac{5}{37}\right)\left(\frac{32}{37}\right) + \left(\frac{32}{37}\right)\left(\frac{5}{37}\right) = 0.23.$$

The following conclusions can be drawn from Figures 6 and 7:

1. Spectrogram correlation using seven principal components is superior to the other algorithms that were tested for Pr [misclassification] $\leq$ 0.1. For spectrogram analysis, probability of misclassification drops below 0.1 for SNR greater than -5 dB to 0 dB for a white noise background, and for SCR greater than 1 dB to 6 dB for a background of bottom clutter.

2. The addition of a timing parameter to the bionic component (or geometrical theory of diffraction) method is helpful for a white noise background for SNR > 0 dB, but the timing parameter makes little difference in clutter or in white noise with SNR < 0 dB. Performance of the five-component GTD method seems to be roughly the same in noise and reverberation, but the spectrogram method does worse in reverberation than it does in white noise.

3. The Fourier-Mellin representation, FM-gram, has larger storage requirements than the spectrogram method, since more principal components must be used. The relative performance of FM-gram in white noise is quite poor, but the performance is better in clutter. In any case, FM-gram is generally inferior to the spectrogram method.

Since the spectrogram correlator with seven principal components was found to be superior, one may wonder whether even better performance can be obtained with more components. Table 4 shows the performance of the spectrogram correlator at 0 dB SCR and 0 dB SNR for five, seven, and nine principal components. The table indicates that very little improvement will be obtained by using more than seven components for spectrogram analysis.

Table 4. Performance of the spectrogram correlator at 0 dB SNR or 0 dB SCR for 5, 7, and 9 principal components

| Classification problem | | Number of components | | |
|---|---|---|---|---|
| | | 5 | 7 | 9 |
| Pr [Misclassification, 2.5 x 7" Al. cyl. vs. other targets] | in noise (0 dB SNR) | 0.17 | 0.10 | 0.093 |
| | in reverb. (0 dB SCR) | 0.32 | 0.27 | 0.25 |
| Pr [Misclassification, cylindrical vs. non-cylindrical targets] | in noise (0 dB SNR) | 0.073 | 0.051 | 0.048 |
| | in reverb. (0 dB SCR) | 0.14 | 0.14 | 0.13 |
| Pr [Misclassification, metal vs. non-metal targets] | in noise (0 dB SNR) | 0.058 | 0.055 | 0.052 |
| | in reverb. (0 dB SCR) | 0.12 | 0.12 | 0.12 |

## 1.6 Conclusion

The best software algorithm to date is a spectrogram correlator that uses principal component analysis. For a single pulse, this processor gives a 0.1 probability of misclassification for a worst-case signal-to-clutter ratio of 6 dB. If multiple pulses are used, the noise component of the measured clutter process will be reduced. The effect of the clutter itself can be reduced if a target can be viewed from a sequence of different aspect angles, since different bottom reflections will be encountered at each aspect, and the clutter echoes will be more noise-like or random. The results of Figure 7a indicate that a small aluminum cylinder can be distinguished from other targets even when the aspect of the cylinder is varied. Additional pulses and "look" angles can therefore be expected to further improve performance in an operational environment.

The use of a spectrogram correlation process for detection of range-distributed targets can be defended from three different viewpoints:

1. It works better than anything we have tried thus far.
2. A spectrogram representation is apparently a good approximation to the representation of auditory data that is passed to the central nervous system in mammals (Volume 2, Chapters 2.2 and 2.3).
3. Spectrogram correlation is equivalent to optimum Bayes or Neyman-Pearson detection for range-distributed targets at low signal-to-noise ratio (Volume 2, Chapter 2.4).

The spectrogram correlator as an optimum detector and as a model for auditory signal processing is discussed in Volume 2.

## 1.7 References for Volume 1.


1. H. C. Andrews, Introduction to Mathematical Techniques in Pattern Recognition, New York: Wiley-Interscience, 1972.

2. R. G. Kouyoumjian, "Asymptotic high-frequency methods," Proc. IEEE, vol. 53, pp. 864-876, 1965.

3. M. E. Bechtel, "Application of geometric diffraction theory to scattering from cones and disks," Proc. IEEE, vol. 53,

4. M. E. Bechtel, "Short pulse target characteristics," in Proc. NATO Adv. Study Inst. on Atmos. Effects on Radar Target Ident. and Imaging, H. E. G. Jeske (ed.), pp. 3-53, Dordrecht: D. Reidel, 1975.

5. D. M. Chabries, "High frequency acoustic scattering," NUC Technical Report, June 1975.

6. J. B. Keller, "Geometrical theory of diffraction," J. Opt. Soc. Amer., vol. 52, pp. 116-130, 1962.

7. T. B. A. Senior, "A survey of analytical techniques for cross-section estimation," Proc. IEEE, vol. 53, pp. 822-833, 1965.

8. M. E. Bechtel, and R. A. Ross, "Radar scattering analysis," CAL report no. ER/RIS-10, Aug. 1966, Cornell Aeronautical Lab., Buffalo, New York.

9. F. M. Tesche, "On the analysis of scattering and antenna problems using the singularity expansion technique," IEEE Trans. on Antennas and Prop., vol. AP-21, pp. 53-62, 1973.

10. L. Marin, and R. W. Latham, "Representation of transient scattered fields in terms of free oscillations of bodies," Proc. IEEE (lettr.), vol. 60, pp. 640-641, 1972.

11. E. K. Miller, et al., "Radar target classification using temporal mode analysis," Lawrence Livermore Lab., Univ. of California, Livermore, CA 94550, Report UCRL-51825, 27 May 1975.

12. R. H. Schafer and R. G. Kouyoumjian, "Transient currents on a cylinder illuminated by an impulsive plane wave," IEEE Trans. on Antennas and Prop., vol. AP-23, pp. 627-638, 1975.

13. D. A. Hill, "Electromagnetic scattering concepts applied to the detection of targets near the ground," Ohio State Univ. Electroscience Lab. Report 2971-1, Air Force Cambridge Res. Lab. Report AFCRL-70-0250.

14. R. A. Altes, "Advances in bionic sonar," SAI-78-539-LJ, Science Applications, Inc., January 1978.

15. R. A. Altes, "Sonar for generalized target description," J. Acous. Soc. Am. 59, pp. 97-105, 1976.

16. T. Kailath, "Correlation detection of signals perturbed by a random channel, "IRE Trans. on Inform. Theory IT-6, pp. 361-366, 1960.

17. E. Zwicker, "Subdivision of the audible frequency range into critical bands," J. Acous. Soc. Am. vol. 33, p. 248, 1961.

18. R. R. Pfeiffer and D. O. Kim, "Cochlear nerve fiber responses: distribution along the cochlear partition," J. Acous. Soc. Am. vol. 58, pp. 867-869, 1975.

19. E. F. Evans, "Peripheral processing of complex sounds," in Recognition of Complex Acoustic Signals, T. H. Bullock (ed.), Abakon Verlagsgesellschaft, Berlin, pp. 145-159, 1977.

20. E. F. Evans, "Cochlear nerve and cochlear nucleus," in Handbook of Sensory Physiology, vol. V, part II, W. D. Keidel and W. D. Neff (eds.), Springer-Verlag, Berlin, pp. 1-108, 1975.

21. W. M. Siebert, "Stimulus transformations in the peripheral auditory system," in Recognizing Patterns, P. A. Kolers and M. Eden (eds.), Cambridge, MA, MIT Press, pp. 104-133, 1968.

22. E. de Boer, "Syntheti c whole-nerve action potentials for the cat," J. Acous. Soc. Am. vol. 58, pp. 1030-1045, 1975.

23. W. M. Siebert, "Frequency discrimination in the auditory system: place or periodicity mechanisms?" Proc. IEEE, vol. 58, pp. 723-730, 1970.

24. R. Srinivasan, "Auditory critical bandwidth for short-duration signals," J. Acous. Soc. Am. vol. 50, pp. 616-622, 1971.

25. D. M. Green, "Auditory detection of a noise signal," J. Acous. Soc. Am. vol. 32, pp. 121-131, 1960.

26. R. A. Johnson and E. L. Titlebaum, "Energy spectrum analysis: a model of echolocation processing," J. Acous. Soc. Am. vol. 60, pp. 484-491, 1976.

27. Y. T. Chien and K. S. Fu, "Selection and ordering of feature observations in a pattern recognition system," Inform. and Control. vol. 12, pp. 395-414, 1968.

28. H. G. Nilsson, "A comparison of models for sharpening of the frequency selectivity in the cochlea," Biol. Cybernetics, vol. 28, pp. 177-181, 1978.

29. D. W. Sparks, "Temporal recognition masking – or interference?" J. Acous. Soc. Am. vol. 60, pp. 1347-1353, 1976.

30. D. H. Hubel and T. N. Wiesel, "Receptive fields and functional architecture of monkey striate cortex," J. Physiol. (London), vol. 195, pp. 215-243, 1968.

31. R. A. Altes, "The Fourier-Mellin transform and mammalian hearing," J. Acous. Soc. Am. vol. 63, pp. 174-183, 1978.

32. R. A. Altes, "Mechanism for aural pulse compression in mammals," J. Acous. Soc. Am. vol. 57, pp. 513-515, 1975.

33. J. J. Kroszczynski, "Pulse compression by means of linear-period modulation," Proc. IEEE, vol. 57, pp. 1260-1266, 1969.

34. D. A. Cahlander, "Echolocation with wide-band waveforms," AD 605332.

35. R. A. Altes and W. D. Reese, "Doppler tolerant classification," IEEE Trans. on Aerospace and Electronic Systems, AES-11, pp. 708-724, 1975.

36. R. H. Kay and D. R. Mathews, "On the existence in human auditory pathways of channels selectively tuned to the modulation present in frequency-modulated tones," J. Physiol. vol. 225, pp. 657-677, 1972.

37. R. F. Daly, "Signal design for efficient detection in dispersive channels," IEEE Trans. on Inform. Theory, IT-16, pp. 206-213, 1970.

1.8 Appendices for Volume 1.

APPENDIX A: FORTRAN PROGRAM FOR CONSTRUCTION OF A SHORT-DURATION SPECTROGRAM

```
C
C*****  MAIN ALTES.SGRAM1
C
C
C
C       SITE -- NOSC, SAN DIEGO
C       MACHINE -- UNIVAC 1110
C       COMPILER - FTN(ASCII) FORTRAN   15 AUG 1978
C       EXT. LIBRARIES:
C
C       ALTES.
C       N*FTNLIB.
C
C*****  FUNCTION:
C
C       COMPUTE SPECTROGRAMS OF TARGET ECHO PLUS NOISE SAMPLES
C
C
C*****  PROCESS CONTROL PARAMETERS:
C
C     PARAMETER                                   USAGE
C
C       NTARG               NUMBER OF TARGET ECHOS TO BE PROCESSED
C                           (D=38, R=1-38)
C
C       MTARG(I)            RECORD POSITION IN RAN ACCESS FILE OF
C                           I'TH TARGET (D=I, R=1-38)
C
C       SCI                 SIGNAL COMPOSITION INDEX
C                           IF(SCI=1) SIGNAL: SF*ECHO+NOISE
C                           IF(SCI=0) SIGNAL: ECHO
C                           IF(SCI=-1) SIGNAL: NOISE
C
C       NSMP                NUMBER OF NOISE SAMPLES TO BE USED
C                           PER TARGET
C
C       RNIO                LABEL OF FIRST NOISE SAMPLE.  SEQUENTIAL
C                           ACCESS IS USED THEREAFTER. (D=1)
C
C       NSNR                NUMBER OF SIGNAL TO NOISE RATIOS TO USE
C                           PER TARGET PER NOISE SAMPLE (D=6, R=1-6)
C
C       ASNR(I)             VALUE OF THE I'TH SIGNAL TO NOISE RATIO
C                           (D=SEE DATA STATEMENT)
C
```

APPENDIX A (continued)

```
C       LDSPLA              LOGICAL VARIABLE INDICATES WHETHER SPECTRO-
C                           GRAM IS TO BE DISPLAYED (=T) OR NOT (=F)
C                           (D=F)
C
C*****   FILES
C
C     FILE                    USE
C
C     TEF/9         - INPUT TARGET ECHO FILE
C     NF/3          - INPUT NOISE FILE
C     FMF/8         - INPUT MATCHED FILTER FILE
C     RF/10         - OUTPUT RESULTS FILE
C     CARDS/5       - INPUT CARD FILE
C     PRINTER/6     - OUTPUT PRINT FILE
C
C
C*****  DATA STRUCTURE ELEMENTS
C
C
      DIMENSION ASNR(10),ECHO(1024),EPN(1024),ENG(300),W(32),
     1SPCG(28,16),ISPCG(28,16)
      INTEGER MTARG(38),SCI,TEF,FMF,RF
      REAL NOIS(1024)
      COMPLEX SMF(512),CEPN(1024),F(32)
      LOGICAL LDSPLA
C
C*****  NAMELIST, DATA STATEMENTS, FORMATS, ETC.
C
C
      NAMELIST/CARDS/NTARG,MTARG,SCI,NSMP,RNIO,NSNR,ASNR,LDSPLA
      DATA (ASNR(I), I=1,6)/100.,20.,10.,4.,2.,1./
    1 FORMAT(///5X,'ERROR - TARGET NUMBER ',I3,' REQUESTS ',
     *'RECORD ',I3)
    2 FORMAT(//10X,'RUN SPECIFICATION'//
     *5X,'NO. OF ECHOS',T40,I10,T55,'NTARG'/
     *5X,'SIGNAL COMPOSITION INDEX',T40,I10,T55,'SCI'/
     *5X,'INITIAL NOISE SEQUENCE TAG',T40,F10.0,T55,'RNIO'/
     *5X,'NO. OF SAMPLES PER ECHO',T40,I10,T55,'NSMP'/
     *5X,'NO. OF SNRS PER SAMPLE',T40,I10,T55,'NSNR')
C
C*****  1.1   -  SET PROCESS CONTROL PARAMETER & DEFAULT VALUES;
C               READ CONTROL PARAMETERS; READ SIGNAL MATCHED
C               FILTER
C
C
      NTARG=38
      DO 100 I=1,38
      MTARG(I)=I
  100 CONTINUE
```

APPENDIX A (continued)

```
      SCI=1
      NF=3
      RF=10
      TEF=9
      FMF=8
      RNIO=1.
      NSNR=6
      LDSPLA=.FALSE.
      RNI=0.
      READ(5,CARDS,END=110)
  110 CONTINUE
      READ(FMF)(SMF(I), I=1,512)
      IF(SCI.EQ.1)GO TO 140
      IF(SCI.EQ.-1)GO TO 120
      ASNR(1)=1.E30
      NSMP=1
      GO TO 130
  120 CONTINUE
      ASNR(1)=0.
      NTARG=1
  130 CONTINUE
      NSNR=1
  140 CONTINUE
      WRITE(6,2)NTARG,SCI,RNIO,NSMP,NSNR
C
C*****  1.2  BEGIN TARGET ECHO LOOP
C
C     INITIAL CONDITION- ITARG=1
C     TERMINATION CONDITION - ITARG>NTARG
C     RETURN POINT LABEL - 200
C     EXIT POINT LABEL - 620
C
C
      DEFINE FILE 9(38,1024,U,N9)
      ITARG=1
  200 CONTINUE
      IF(ITARG.GT.NTARG)GO TO 620
C
C*****  2.1  READ TARGET ECHO IF REQUIRED
C
C
      IF(SCI.GE.0)GO TO 210
      NER=0
      DO 205 I=1,1024
      ECHO(I)=0.
  205 CONTINUE
      GO TO 220
  210 CONTINUE
```

APPENDIX A (continued)

```
      NER=MTARG(ITARG)
      IF(NER.LE.38.AND.NER.GE.1)GO TO 215
      WRITE(6,1)ITARG,NER
      STOP
  215 CONTINUE
      READ(TEF'NER)ECHO
  220 CONTINUE
C
C*****  2.2  BEGIN NOISE SAMPLE LOOP
C
C     INITIAL CONDITION - ISMP=1
C     TERMINATION CONDITION - ISMP>NSMP
C     RETURN POINT LABEL - 300
C     EXIT POINT LABEL - 610
C
C
      ISMP=1
  300 CONTINUE
      IF(ISMP.GT.NSMP)GO TO 610
C
C*****  3.1  READ NOISE SAMPLE IF REQUIRED
C
C
      IF(SCI.EQ.0)GO TO 310
      CALL RDNOIS(NF,NOIS,RNI,RNIO)
      GO TO 330
  310 CONTINUE
      DO 320 I=1,1024
      NOIS(I)=0.
  320 CONTINUE
  330 CONTINUE
C
C*****  3.2  BEGIN SIGNAL TO NOISE RATIO LOOP
C
C     INITIAL CONDITION - ISNR=1
C     TERMINATION CONDITION - ISNR>NSNR
C     RETURN POINT LABEL - 400
C     EXIT POINT LABEL - 600
C
C
      ISNR=1
  400 CONTINUE
      IF(ISNR.GT.NSNR)GO TO 600
      SNR=ASNR(ISNR)
C
C*****  4.1  MIX ECHO AND NOISE BY SNR AND PASS THRU
C           FILTER MATCHED TO SIGNAL
C
C
```

APPENDIX A (continued)

```
      INR=SNR
      IF(SCI.EQ.0)INR=1.
      CALL ENMIX(ECHO,NOIS,INR,EPN)
      DO 410 I=1,1024
      CEPN(I)=CMPLX(EPN(I),0.)
  410 CONTINUE
      CALL RFFT(CEPN,1024,10,0)
      DO 420 I=1,512
      CEPN(I)=CEPN(I)*SMF(I)
  420 CONTINUE
C
C*****  4.2  LOW PASS FILTER RESPONSE TO 56 KHZ AND
C            RETURN TO TIME DOMAIN AND SAMPLE RESPONSE
C
      DO 430 I=116,1024
      CEPN(I)=CMPLX(0.,0.)
  430 CONTINUE
      CEPN(114)=CEPN(114)*CMPLX(.5886,0.)
      CEPN(115)=CEPN(115)*CMPLX(.1065,0.)
      CALL RFFT(CEPN,1024,10,1)
      K=0
      DO 440 I=4,1024,4
      K=K+1
      EPN(K)=REAL(CEPN(I))
  440 CONTINUE
C
C*****  4.3  SMOOTH ENERGY FUNCTION AND LOCATE MAX
C
C
      SUM2=0.
      DO 450 I=1,16
      SUM2=SUM2+EPN(I)**2
  450 CONTINUE
      ENG(1)=SUM2
      EMAX=ENG(1)
      KMAX=1
      DO 470 I=2,256
      K=I+15
      IF(K.GT.256)K=K-256
      SUM2=SUM2+EPN(K)**2-EPN(I-1)**2
      IF(SUM2.LE.EMAX)GO TO 460
      EMAX=SUM2
      KMAX=I
  460 CONTINUE
      ENG(I)=SUM2
  470 CONTINUE
C
```

APPENDIX A (continued)

```
C*****  4.4  CONSTRUCT SPECTROGRAM: WINDOW DATA IN
C            TIME DOMAIN; TRANSFORM OVERLAPPED SEGMENTS
C
C
      DO 500 I=1,15
      X=I-8.5
      W(I)=.5*(1.+COS(3.14159*X/7.5))
  500 CONTINUE
      DO 510 I=16,32
      ENG(I)=0.
  510 CONTINUE
      DO 550 IND=1,28
      IS=KMAX+(IND-1)*3-32
      DO 515 I=1,15
      J=IS+I
      IF(J.LT.1)J=J+256
      IF(J.GT.256)J=J-256
      ENG(I)=W(I)*EPN(J)
  515 CONTINUE
      DO 520 I=1,32
      F(I)=CMPLX(ENG(I),0.)
  520 CONTINUE
      CALL RFFT(F,32,5,0)
      DO 550 I=1,16
      SPCG(IND,I)=F(I)*CONJG(F(I))
  550 CONTINUE
      SMAX=0.
      DO 560 N=1,28
      DO 560 I=1,16
      SMAX=AMAX1(SPCG(N,I),SMAX)
  560 CONTINUE
      DO 570 N=1,28
      DO 570 I=1,16
      SPCG(N,I)=SPCG(N,I)*99./SMAX
      ISPCG(N,I)=SPCG(N,I)
  570 CONTINUE
C
C*****  4.5  WRITE RESULTS TO OUTPUT FILE AND DISPLAY
C            IF LDSPLA=T
C
C
      WRITE(RF)NER,SNR,RNI,((SPCG(J,I), J=1,28,2), I=1,16)
      IF(LDSPLA)CALL DSPLA(NER,SNR,RNI,ISPCG)
      ISNR=ISNR+1
      GO TO 400
C
C*****  3.3  END SIGNAL TO NOISE RATIO LOOP
```

APPENDIX A (concluded)

```
C
C
  300 CONTINUE
      ISMP=ISMP+1
      GO TO 300
C
C*****  2.3  END NOISE SAMPLE LOOP
C
C
  610 CONTINUE
      ITARG=ITARG+1
      GO TO 200
C
C*****  1.3  END TARGET ECHO LOOP
C
C
  620 CONTINUE
      ENDFILE RF
      ENDFILE RF
      END
```

## APPENDIX B: FORTRAN PROGRAM FOR GENERATING FM-GRAM

```
C
C*****  MAIN ALTES.FGRAM1
C
C
C       SITE -- NOSC, SAN DIEGO
C       MACHINE -- UNIVAC 1110
C       COMPILER -- FTN(ASCII) FORTRAN  21 AUG 1978
C       EXT. LIBRARIES:
C
C       ALTES.
C       N*FTNLIB.
C
C*****  FUNCTION:
C
C       FORMS A MODIFIED SPECTROGRAM THAT IS BASED
C       UPON MATCHED FILTERS WITH DIFFERENT LOG
C       CHIRP FACTORS
C
C*****  PROCESS CONTROL PARAMETERS
C
C     PARAMETER                                 USAGE
C
C       NTARG                 NUMBER OF TARGET ECHOS TO BE PROCESSED
C                             (D=38, R=1-38)
C
C       MTARG(I)              RECORD POSITION IN RAN ACCESS FILE OF
C                             I'TH TARGET (D=I, R=1-38)
C
C       SCI                   SIGNAL COMPOSITION INDEX
C                             IF(SCI=1) SIGNAL: SF*ECHO+NOISE
C                             IF(SCI=0) SIGNAL: ECHO
C                             IF(SCI=-1) SIGNAL: NOISE
C
C       NSMP                  NUMBER OF NOISE SAMPLES TO BE USED
C                             PER TARGET
C
C       RNIO                  LABEL OF FIRST NOISE SAMPLE.  SEQUENTIAL
C                             ACCESS IS USED THEREAFTER. (D=1)
C
C       NSNR                  NUMBER OF SIGNAL TO NOISE RATIOS TO USE
C                             PER TARGET PER NOISE SAMPLE (D=6, R=1-6)
C
C       ASNR(I)               VALUE OF THE I'TH SIGNAL TO NOISE RATIO
C                             (D=SEE DATA STATEMENT)
C
C       LDSPLA                LOGICAL VARIABLE INDICATES WHETHER SPECTRO-
C                             GRAM IS TO BE DISPLAYED (=T) OR NOT (=F)
C                             (D=F)
```

APPENDIX B (continued)

```
C
C
C*****   FILES
C
C     FILE                    USE
C
C     TEF/9            - INPUT TARGET ECHO FILE
C     NF/3             - INPUT NOISE FILE
C     RF/10            - OUTPUT RESULTS FILE
C     CARDS/5          - INPUT CARD FILE
C     PRINTER/6        - OUTPUT PRINT FILE
C
C
C*****  DATA STRUCTURE ELEMENTS
C
      DIMENSION ASNR(15),ECHO(1024),RESP(7,256),EPN(1024),IRESP(7,100),
     1RESP1(7,100)
      INTEGER MTARG(38),RF,SCI,TEF
      REAL NOIS(1024)
      COMPLEX U(7,128),V(256),DD(256)
      LOGICAL LDSPLA
C
C*****  NAMELIST, DATA STATEMENTS, FORMATS, ETC.
C
C
      DEFINE FILE 9(38,1024,U,N9)
      NAMELIST /CARDS/NTARG,MTARG,SCI,NSMP,RNIO,NSNR,ASNR,LDSPLA
      DATA (ASNR(I), I=1,6)/100.,20.,10.,4.,2.,1./
    1 FORMAT(///5X,'ERROR - RECORT NUMBER ',I2,' REQUESTS ',
     *'RECORD ',I3)
    2 FORMAT(//10X,'RUN SPECIFICATION'//
     *5X,'NO. OF ECHOS',T40,I10,T55,'NTARG'/
     *5X,'SIGNAL COMPOSITION INDEX',T40,I10,T55,'SCI'/
     *5X,'INITIAL NOISE SEQUENCE TAG',T40,F10.0,T55,'RNIO'/
     *5X,'NO. OF SAMPLES PER ECHO',T40,I10,T55,'NSMP'/
     *5X,'NO. OF SNRS PER SAMPLE',T40,I10,T55,'NSNR'/
     *5X,'S/N RATIOS',T40,E10.4,T55,'ASNR(I)'/
     *14(T40,E10.4/))
C
C*****  SET PROCESS CONTROL PARAMETERS AND DEFAULT VALUES
C
C       READ CONTROL PARAMETERS
C
      NTARG=38
      DO 100 I=1,38
      MTARG(I)=I
  100 CONTINUE
```

APPENDIX B (continued)

```
      SCI=1
      TEF=9
      NF=3
      RF=10
      RNIO=1.
      NSNR=6
      LDSPLA=.FALSE.
      RNI=0.
      READ(5,CARDS,END=110)
  110 CONTINUE
      IF(SCI.EQ.1)GO TO 140
      IF(SCI.EQ.-1)GO TO 120
      ASNR(1)=1.E30
      NSMP=1
      GO TO 130
  120 CONTINUE
      ASNR(1)=0.
      NTARG=1
  130 CONTINUE
      NSNR=1
  140 CONTINUE
      WRITE(6,2)NTARG,SCI,RNIO,NSMP,NSNR,(ASNR(J),J=1,NSNR)
C
C*****  COMPUTE 'MATCHED' FILTERS WITH RANGE OF CHIRP FACTORS.
C
C
      S=47.
      FK=1.2
      FC=-.25
      WN=1./(2.*ALOG(FK))
      W=0.
      DO 160 N=1,7
      DO 160 I=1,128
      IF(I.LT.10 .OR. I.GT.127)GO TO 150
      X2=(I-1.)/S
      Y1=ALOG(X2)
      Y5=1./X2
      IF(I.EQ.10 .OR. I.EQ.127)Y5=0.1065*Y5
      IF(I.EQ.11 .OR. I.EQ.126)Y5=0.5886*Y5
      CHRP=N-3.
      Z=2.*WN*6.2832*Y1*FC*CHRP
      CN=COS(Z)
      SN=SIN(Z)
      Y6=Y5*CN
      Y7=Y5*SN
      U(N,I)=CMPLX(Y6,-Y7)
      GO TO 160
  150 CONTINUE
```

APPENDIX B (continued)

```
      U(N,1)=CMPLX(0.,0.)
  160 CONTINUE
C
C*****  BEGIN TARGET ECHO LOOP
C
C INITIAL CONDITION - ITARG=1
C TERMINATION CONDITION - ITARG>NTARG
C RETURN POINT LABEL - 200
C EXIT POINT LABEL - 620
C
C
      ITARG=1
  200 CONTINUE
      IF(ITARG.GT.NTARG)GO TO 620
C
C*****  READ TARGET ECHO IF REQUIRED
C
C
      IF(SCI.GE.0)GO TO 210
      NER=0
      DO 205 I=1,1024
      ECHO(I)=0.
  205 CONTINUE
      GO TO 220
  210 CONTINUE
      NER=MTARG(ITARG)
      IF(NER.LE.38.AND.NER.GE.1)GO TO 215
      WRITE(6,1)ITARG,NER
      STOP
  215 CONTINUE
      READ(TEF'NER)ECHO
  220 CONTINUE
C
C*****  BEGIN NOISE SAMPLE LOOP
C
C INITIAL CONDITION - ISMP=1
C TERMINATION CONDITION - ISMP>NSMP
C RETURN POINT LABEL - 300
C EXIT POINT LABEL - 610
C
C
      ISMP=1
  300 CONTINUE
      IF(ISMP.GT.NSMP)GO TO 610
C
C*****  READ NOISE TARGET IF REQUIRED
C
C
```

APPENDIX B (continued)

```
      IF(SCI.EQ.0)GO TO 310
      CALL RDNOIS(NF,NOIS,RNI,RNIO)
      GO TO 330
  310 CONTINUE
      DO 320 I=1,1024
      NOIS(I)=0.
  320 CONTINUE
  330 CONTINUE
C
C*****  BEGIN SIGNAL TO NOISE RATIO LOOP
C
C INITIAL CONDITION - ISNR=1
C TERMINATION CONDITION - ISNR>NSNR
C RETURN POINT LABEL - 400
C EXIT POINT LABEL - 600
C
      ISNR=1
  400 CONTINUE
      IF(ISNR.GT.NSNR)GO TO 600
      SNR=ASNR(ISNR)
C
C*****  MIX ECHO AND NOISE BY SNR
C
C
      TNR=SNR
      IF(SCI.EQ.0)TNR=1.
      CALL ENMIX(ECHO,NOIS,TNR,EPN)
C
C*****  COMPUTE TRANSFORM OF SAMPLED SIGNAL
C
C
      DO 410 I=1,256
      K=4*I
      DD(I)=CMPLX(EPN(K),0.)
  410 CONTINUE
      DO 420 I=1,256
      EPN(I)=REAL(DD(I))
  420 CONTINUE
      CALL RFFT(DD,256,8,0)
C
C*****  COMPUTE 'MATCHED' FILTER RESPONSES.
C
C
      DO 450 N=1,7
      DO 430 I=1,128
      V(I)=U(N,I)*DD(I)
      V(I+128)=CMPLX(0.,0.)
  430 CONTINUE
```

**APPENDIX B (continued)**

```
      CALL RFFT(V,256,8,1)
      DO 440 I=1,256
      RESP(N,I)=CABS(V(I))**4
  440 CONTINUE
  450 CONTINUE
C
C*****  NORMALIZE RESPONSES
C
C
      RMAX=0.
      IMAX=0
      DO 460 N=1,7
      DO 460 I=1,256
      IF(RESP(N,I).LE.RMAX)GO TO 460
      IMAX=I
      RMAX=RESP(N,I)
  460 CONTINUE
      DO 470 N=1,7
      DO 470 I=1,256
      RESP(N,I)=RESP(N,I)*99./RMAX
  470 CONTINUE
      IBEG=IMAX-49
      IEND=IMAX+50
      K=1
      DO 480 I=IBEG,IEND
      DO 475 N=1,7
      J=I-8*(N-4)
      IF(J.LT.1)J=J+256
      IF(J.GT.256)J=J-256
      RESP1(N,K)=RESP(N,J)
      IRESP(N,K)=RESP1(N,K)
  475 CONTINUE
      K=K+1
  480 CONTINUE
C
C*****  WRITE RESULTS TO OUTPUT FILE AND
C       DISPLAY IF LDSPLA=T
C
      WRITE(RF)NER,SNR,RNI,((RESP1(N,I), I=1,100,2), N=1,7)
      IF(LDSPLA)CALL DSPLA(NER,IRESP)
      ISNR=ISNR+1
      GO TO 400
C
C******  END SIGNAL TO NOISE RATIO LOOP
C
C
  600 CONTINUE
      ISMP=ISMP+1
      GO TO 300
```

APPENDIX B (concluded)

```
C
C*****  END NOISE SAMPLE LOOP
C
C
  610 CONTINUE
      ITARG=ITARG+1
      GO TO 200
C
C*****  END TARGET ECHO LOOP
C
C
  620 CONTINUE
      END
```